(12) INTERNATIONAL APPLICATION PUBLISHED UNDER THE PATENT COOPERATION TREATY (PCT)

(19) World Intellectual Property Organization
International Bureau

(43) International Publication Date
24 October 2024 (24.10.2024)

WIPO | PCT

(10) International Publication Number
WO 2024/220554 A2

(51) International Patent Classification:
Not classified

(21) International Application Number:
PCT/US2024/025011

(22) International Filing Date:
17 April 2024 (17.04.2024)

(25) Filing Language: English

(26) Publication Language: English

(30) Priority Data:
63/459,738 17 April 2023 (17.04.2023) US

(71) Applicant: **THE GENERAL HOSPITAL CORPORATION** [US/US]; 55 Fruit Street, Boston, MA 02114 (US).

(72) Inventors: **IM, Hyungsoon**; 56 Forest Ridge Road, Weston, MA 02493 (US). **HONG, Jaesang**; 64 Hastings Street, Apt 108, Wellesley, MA 02481 (US).

(74) Agent: **DECAMP, James, D.** et al.; Clark & Elbing LLP, 101 Federal Street, 15th Floor, Boston, MA 02110 (US).

(81) Designated States *(unless otherwise indicated, for every kind of national protection available)*: AE, AG, AL, AM, AO, AT, AU, AZ, BA, BB, BG, BH, BN, BR, BW, BY, BZ, CA, CH, CL, CN, CO, CR, CU, CV, CZ, DE, DJ, DK, DM, DO, DZ, EC, EE, EG, ES, FI, GB, GD, GE, GH, GM, GT, HN, HR, HU, ID, IL, IN, IQ, IR, IS, IT, JM, JO, JP, KE, KG, KH, KN, KP, KR, KW, KZ, LA, LC, LK, LR, LS, LU, LY, MA, MD, MG, MK, MN, MU, MW, MX, MY, MZ, NA, NG, NI, NO, NZ, OM, PA, PE, PG, PH, PL, PT, QA, RO, RS, RU, RW, SA, SC, SD, SE, SG, SK, SL, ST, SV, SY, TH, TJ, TM, TN, TR, TT, TZ, UA, UG, US, UZ, VC, VN, WS, ZA, ZM, ZW.

(84) Designated States *(unless otherwise indicated, for every kind of regional protection available)*: ARIPO (BW, CV, GH, GM, KE, LR, LS, MW, MZ, NA, RW, SC, SD, SL, ST, SZ, TZ, UG, ZM, ZW), Eurasian (AM, AZ, BY, KG, KZ, RU, TJ, TM), European (AL, AT, BE, BG, CH, CY, CZ, DE, DK, EE, ES, FI, FR, GB, GR, HR, HU, IE, IS, IT, LT, LU, LV, MC, ME, MK, MT, NL, NO, PL, PT, RO, RS, SE, SI, SK, SM, TR), OAPI (BF, BJ, CF, CG, CI, CM, GA, GN, GQ, GW, KM, ML, MR, NE, SN, TD, TG).

Declarations under Rule 4.17:
— *as to applicant's entitlement to apply for and be granted a patent (Rule 4.17(ii))*
— *of inventorship (Rule 4.17(iv))*

Published:
— *without international search report and to be republished upon receipt of that report (Rule 48.2(g))*

(54) Title: MICRO RNA DETECTION IN TUMOR DERIVED EXTRACELLULAR VESICLES

(57) Abstract: The invention features methods and compositions for detection of an miRNA biomarker in an extracellular vesicle (e.g., a tumor-derived EV).

WO 2024/220554 A2

MICRO RNA DETECTION IN TUMOR DERIVED EXTRACELLULAR VESICLES

CROSS-REFERENCE TO RELATED APPLICATION

This application claims the benefit of U.S. Patent Application Serial No. 63/459,738, filed on April 17, 2023. The disclosure of the prior application is considered part of (and is incorporated by reference in) the disclosure of this application.

STATEMENT AS TO FEDERALLY FUNDED RESEARCH

This invention was made with government support under 5R21CA217662-03 awarded by the NIH-NCI and under 5R01GM138778-03 awarded by the NIH-NIGMS. The government has certain rights in the invention.

BACKGROUND OF THE INVENTION

Extracellular vesicles (EVs) are nano-sized secretory particles originating from the cellular endosomal trafficking system. EVs contain molecular cargo, including common and cell-specific proteins, nucleic acids, and lipids, reflecting the physiological characteristics of cells of origin. This property makes EVs attractive as circulating biomarkers. Among various molecules contained in EVs, microRNAs (miRNAs) are a group of small non-coding RNAs involved in post-transcriptional gene regulation by inhibiting translation and cleavage of their target RNA transcripts. miRNAs are involved in many biological processes, such as cell development, apoptosis, cell proliferation, immune response, and tumorigenesis, through intercellular communications via EVs.

Recent studies have demonstrated the different roles of EV miRNAs. First, miRNAs are involved in disease initiation and progression. Thus, up- or down-regulation of specific miRNA can be used as a diagnostic marker for cancers, cardiovascular diseases, lung diseases, and neurodegenerative diseases, among many others. Second, EV miRNAs play essential roles in cell-to-cell communications. For instance, a lymphocyte-specific miRNA, miR-150, released from THP1 cell-derived EVs was delivered into the human microvascular endothelial HMEC-1 cells, which resulted in the enhancement of cell migration by modulating c-Myb expression. Therefore, accurate, quantitative measurements of EV miRNAs become critical for the clinical translation of the diagnostic biomarkers and a better understanding of EV-medicated biological processes.

Conventional detection methods for EV miRNAs include quantitative reverse transcription polymerase chain reaction (RT-qPCR), northern blotting, microarray, and next-generation sequencing. While these traditional methods are sensitive and provide relative quantification of target miRNAs, all require multiple steps, including EV lysis, RNA extraction, DNase treatment, cDNA synthesis, and amplification. Considering EVs 'high heterogeneity associated with different EV subtypes from almost all kinds of cells, EV lysis eliminates cell-specific information in individual EVs and dilutes miRNAs in a target EV subpopulation by those from non-target subpopulation EVs.

There is a need in the art to detect target miRNAs in intact EVs, which would improve the detection accuracy and pave new ways to investigate RNA biomarkers in different EV subtypes in a multiplexed manner.

SUMMARY OF THE INVENTION

In one aspect, the invention features a liposome including a Cas13a nuclease, a crRNA, and a nucleic acid probe, wherein the nucleic acid probe includes a detectable label, a nucleic acid linker, and a quencher.

In another aspect, the invention features an extracellular vesicle-liposome (EV-liposome) fusion including a Cas13a nuclease, a crRNA, and a nucleic acid probe, wherein the nucleic acid probe includes a detectable label, a nucleic acid linker, and a quencher.

In some embodiments, the EV is a tumor-derived EV.

In some embodiments, the nucleic acid probe includes 5' [detectable label]-[nucleic acid linker]-[quencher] 3'.

In some embodiments, the detectable label is a fluorophore. In some embodiments, the fluorophore includes fluorescein amidite (FAM).

In some embodiments, the nucleic acid linker includes both DNA and RNA nucleotides. In some embodiments, the nucleic acid linker includes DNA-RNA-DNA. In some embodiments, the nucleic acid linker is 5' TAuuGC 3'.

In some embodiments, the quencher is 3' IOWA BLACK® FQ (IABkFQ).

In some embodiments, the nucleic acid probe includes the structure of 5' FAM-TAuuGC- IABkFQ 3'.

In some embodiments, the crRNA is complementary to an miRNA biomarker. In some embodiments, the miRNA biomarker is a cancer biomarker.

In some embodiments, the Cas13a nuclease is LwaCas13a.

In some embodiments, the Cas13a nuclease and the crRNA are present at a concentration of about 100 nM.

In another aspect, the invention features an array including an immobilized capture moiety and a tumor-derived EV.

In some embodiments, the array includes an immobilized capture moiety and a tumor-derived EV-liposome fusion, wherein the EV-liposome fusion includes a Cas13a nuclease, a crRNA, and a nucleic acid probe, and wherein the nucleic acid probe includes a detectable label, a nucleic acid linker, and a quencher.

In some embodiments, the array is a gold microdisk array.

In some embodiments, the array is a gold nanodisk array.

In some embodiments, the array includes a plurality of the immobilized capture moiety. In some embodiments, the immobilized capture moieties on the array are arranged in a grid pattern.

In some embodiments, the immobilized capture moiety is an antibody that specifically binds a tumor-derived EV. In some embodiments, the immobilized capture moiety is an antibody that binds EPCAM.

In some embodiments, the immobilized capture moiety is an antibody that binds a protein over-expressed in solid tumors. In some embodiments, the immobilized capture moiety is an antibody that binds EGFR, MUC1, MUC16, CD24, or HER2.

In some embodiments, the immobilized capture moiety is an antibody that binds a protein associated with drug resistance (for example, chemotherapy resistance). In some embodiments, the immobilized capture moiety is an antibody that binds poly-glycoprotein or survivin.

In another aspect, the invention features a method for detecting an miRNA biomarker in a tumor-derived EV, the method including detecting the miRNA biomarker in an EV-liposome fusion described herein.

In another aspect, the invention features a method for detecting an miRNA biomarker in a tumor-derived EV, including the steps of: (a) providing an array including a plurality of immobilized capture moieties that specifically bind a tumor-derived EV; (b) binding the tumor-derived EVs to the array; (c) incubating the bound tumor-derived EVs with a liposome described herein; and (d) detecting the miRNA biomarker.

In another aspect, the invention features a method for detecting an miRNA biomarker in a tumor-derived EV, including the steps of: (a) providing an array including a plurality of immobilized capture moieties that specifically bind a tumor-derived EV; (b) binding an EV-liposome fusion described herein to the array; and (c) detecting the miRNA biomarker.

In some embodiments, the biomarker is a cancer biomarker.

In some embodiments, the array is a gold microdisk array.

In some embodiments, the array is a gold nanodisk array.

In some embodiments, the array includes a plurality of immobilized capture moieties arranged in a grid pattern.

In some embodiments, the immobilized capture moiety is an antibody that specifically binds a tumor-derived EV. In some embodiments, the immobilized capture moiety is an antibody that binds EPCAM.

In some embodiments, the immobilized capture moiety is an antibody that binds a protein that is over-expressed in solid tumors. In some embodiments, the immobilized capture moiety is an antibody that binds EGFR, MUC1, MUC16, CD24, or HER2.

In some embodiments, the immobilized capture moiety is an antibody that binds a protein associated with drug resistance (for example, chemotherapy resistance). In some embodiments, the immobilized capture moiety is an antibody that binds poly-glycoprotein or survivin.

In some embodiments, the method further includes detecting one or more proteins on the EV-liposome fusion by immunolabeling.

In some embodiments, the one or more proteins are over-expressed in solid tumors. In some embodiments, the one or more proteins includes EGFR, MUC1, MUC16, CD24, or HER2.

In some embodiments, the one or more proteins are associated with drug resistance. In some embodiments, the one or more proteins includes poly-glycoprotein or survivin.

Advantageously, the methods and compositions described herein allow for the detection of protein and miRNA at a single EV level to improve cancer detection accuracy. Previous technologies detect only miRNA or use a general EV marker (CD63) to capture all EVs. Such an approach is not useful for cancer diagnosis, as the tumor-derived EV portion is very small compared to all EVs presented in a plasma sample.

In addition, the methods and compositions described herein allow for target miRNA detection without any target miRNA amplification, while previous technologies used Cas 12 or Cas9, which require target amplification and are prone to false signals or other technical challenges associated with amplifying short miRNA. The methods and compositions of the invention provide a specific miRNA detection method in intact EVs without RNA extraction and allow for multiplexed single EV analysis for protein and RNA markers.

Other features and advantages of the invention will be apparent from the following detailed description and figures, and from the claims.

Definitions

As used herein, the term "about" refers to a value that is within 10% above or below the value being described.

As used herein, the term "array" refers to a substrate including a plurality of nanostructures with one or more immobilized capture moieties fixed on or adjacent to the nanostructures. In some embodiments, the array is a gold microdisk array. In some embodiments, the immobilized capture moieties on the array are arranged in a grid pattern.

As used herein, the term "biomarker" refers to an indicator, e.g., predictive, diagnostic, and/or prognostic, which can be detected in a sample. A biomarker may be an "miRNA biomarker". In some embodiments, the presence or level of an miRNA biomarker in a sample from a subject identifies the subject as having a disorder. In some embodiments, the absence or level of an miRNA biomarker in a sample from a subject identifies the subject as not having a disorder.

The term "capture moiety" as used herein refers to any molecule with the ability to bind to a target (e.g., a tumor-derived EV). Suitable capture moieties include, but are not limited to antibodies or antigen-binding fragments thereof. In some embodiments, the capture moiety may be immobilized on an array.

As used herein, the term "Cas13a nuclease" refers to an RNA-guided RNA nuclease. Exemplary Cas13a nucleases include LwaCas13a, LbaCas13a, and LbuCas13a.

As used herein, the term "CRISPR RNA" or "crRNA" refers to a polynucleotide sequence having sufficient complementarity with a target nucleic acid sequence to hybridize with the target nucleic acid sequence and direct sequence-specific binding of a Cas13a nuclease to the target nucleic acid sequence.

As used herein, the terms "detecting" and "detection" include both qualitative and quantitative measurements of a target molecule. Detecting includes identifying the mere presence of the target molecule in a sample as well as determining whether the target molecule is present in the sample at detectable levels.

As used herein, "detectable label" refers to one or more markers, signals, or moieties which are attached, incorporated or associated to a molecule (e.g., a nucleic acid) which emit an optical signal that is readily detected by methods known in the art including fluorescence, chemiluminescence, absorbance and the like. Detectable labels include fluorophores, radioisotopes, chromophores, enzymes, dyes, ligands such as biotin, avidin, streptavidin and haptens, quantum dots, and the like.

As used herein, "disorder" is used in this disclosure to mean, and is used interchangeably with, the terms condition, disease, or illness, unless otherwise indicated.

As used herein, an "extracellular vesicle" ("EV") refers to nano-sized secretory particles

originating from the cellular endosomal trafficking system. EVs contain molecular cargo, including common and cell-specific proteins, nucleic acids, and lipids, reflecting the physiological characteristics of cells of origin. For example, a "tumor-derived EV" refers to an EV that is released from a tumor cell. EVs include a lipid bilayer membrane enclosing contents of the internal cavity. An EV can include, but is not limited to, an ectosome, a microvesicle, a microparticle, an exosome, an oncosome, an apoptotic body, a liposome, a vacuole, a lysosome, a transport vesicle, a secretory vesicle, a gas vesicle, a matrix vesicle, or a multivesicular body. In some embodiments, the EV may be between about 50 nm to about 250 nm.

As used herein, the term "EV-liposome fusion" refers to a hybrid structure formed from the fusion of an extracellular vesicle and a liposome.

As used herein, "fluorophore" refers to a molecule or complex that can re-emit light upon excitation by an external light source. A fluorophore may absorb light energy and re-emit the energy at a longer wavelength than the absorbed light. Exemplary fluorophores include fluorescein amidite (FAM), fluorescein isothiocyanate (FITC), rhodamine, tetramethylrhodamine isothiocyanate (TRITC), 4',6-diamidino-2-phenylindole (DAPI), coumarin, cyanine, xanthene, naphthalene, oxadiazole, anthracene, pyrene, oxazine, acridine, arylmethine, tetrapyrroles, Alexa Fluor compounds, and BODIPY, or derivatives or conjugates thereof.

As used herein, "fusion" refers to the process by which two initially distinct lipid bilayers merge their hydrophobic cores, resulting in one interconnected structure.

As used herein, the term "lipid nanoparticle" refers to a vehicle including one or more lipids.

As used herein, the term "liposome" refers to an artificially-prepared vesicle including a lipid bilayer.

As used herein, the term "microRNA" or "miRNA" refers to small non-coding RNAs involved in post-transcriptional gene regulation by inhibiting translation and cleavage of their target RNA transcripts. miRNAs are involved in many biological processes, such as cell development, apoptosis, cell proliferation, immune response, and tumorigenesis, through intercellular communications via EVs.

As used herein, the term "nucleic acid probe" refers to a molecule or complex useful for detection of a desired target molecule (e.g., a nucleic acid). A nucleic acid probe of the invention may include a detectable label, a nucleic acid linker, and a quencher.

As used herein, the term "quencher" refers to a molecule that prevents a detectable label from emitting a detectable optical signal. In some embodiments, a quencher prevents a fluorophore from fluorescing. In some embodiments, a quencher may only prevent the fluorophore from fluorescing if the quencher is in close physical proximity to the fluorophore, as is well understood in the art.

As used herein, the term "specific binding" refers to a chemical interaction between two molecules, compounds, cells and/or particles wherein the first entity binds to the second, target entity with greater specificity and affinity than it binds to a third entity which is a non-target. In some embodiments, specific binding can refer to an affinity of the first entity for the second target entity that is at least 10 times greater than the affinity for the third non-target entity.

Unless defined otherwise, all technical and scientific terms used herein have the same meaning as commonly understood to one of ordinary skill in the art to which this disclosure belongs. For any term present in the art which is identical to any term expressly defined in this disclosure, the term's definition presented in this disclosure will control in all respects. Although methods and materials similar or

equivalent to those described herein can be used in the practice of the disclosed methods and compositions, the exemplary methods and materials are described herein.

BRIEF DESCRIPTION OF THE DRAWINGS

The patent or application file contains at least one drawing executed in color. Copies of this patent or patent application with color drawings will be provided by the Office upon request and payment of the necessary fee.

Fig. 1A is a schematic diagram for the CRISPR/Cas13a-based EV miRNA detection assay. Ribonucleoprotein (RNP) complexes (LwaCas13a and miRNA-targeting crRNA) and fluorescence-quencher (FQ) probes are encapsulated in liposomes and delivered to EVs through liposome-EV fusion. crRNA binds to target miRNAs in EVs and activates LwaCas13a. The activated LwaCas13a cleaves FQ probes, generating green fluorescence signals inside EVs. We detect the fluorescence signals co-localized with EV signals and quantify EV counts containing the target miRNA.

Fig. 1B is a graph showing the size distributions of EVs (left), liposomes (middle), and liposome-EV fusion products (right) were measured by nanoparticle tracking analysis.

Fig. 1C is a representative fluorescence image of EV-liposome fusion products showing excellent colocalization of fluorescently labeled EVs (red) and liposomes containing FAM-labeled oligos (green). Scale bar, 100 μm.

Fig. 2 is a Western blot analysis showing the detection of tetraspanins (CD9, CD63, and CD81) in EVs derived from the ES2 ovarian cancer cell line.

Fig. 3 is a representative fluorescence image of fluorescently labeled EVs (red) and cationic liposomes containing fluorescent-conjugated immunoglobulins. Scale bar, 150 μm.

Fig. 4A is an image showing the purification of LwaCas13a confirmed by SDS-PAGE followed by silver staining.

Fig. 4B is an image showing generation and purification of crRNA targeting for miR-21-5p targeting negative control (NC) crRNA with non-complementary sequences to miR-21-5p. The production was assessed by denaturing PAGE and gel staining with SYBR gold.

Fig. 4C is a graph showing the activity of LwaCas13a with different concentrations of miR-21-5p. RNase A and NC crRNA were used as positive and negative controls, respectively.

Fig. 4D is a graph showing the specificity of LwaCas13a-based sensing. Positive fluorescence signals were only generated when target miRNA and complementary crRNA were present.

Fig. 4E is a series of representative fluorescence images of EVs (red, *left*), LwaCas13a-triggered miRNA signals (green, *middle*), and co-localized signals (*right*). Scale bar, 30 μm.

Fig. 4F is a graph showing comparison of miR-21-5p-positive EV counts from the Gli261 wild-type and miR-21 knock-out cell lines. * denotes $P < 0.05$ in the Mann-Whitney test. Bar graphs are shown as mean ± SD ($n = 4$).

Fig. 5A is a graph showing the optimization of the EV miRNA detection assay. Three different parameters (probe sequence, RNP ratio, and RNP concentrations) are optimized for EV miRNA detection.

Fig. 5B is a graph showing comparison of three different linkers between FAM fluorescence probes and quenchers ($n = 4$). The first has only RNA sequences (UUUUU), the second has DNA-RNA-DNA hybrid sequences (TAUUGC), and the third has double quenchers linked with RNA sequences. Bar graphs are shown as mean ± SD, and individual data were plotted as dots. ns, not significant; $^{**}P < 0.01$, $^{****}P < 0.0001$ compared with NC crRNA sample, as assessed by two-way ANOVA with Bonferroni's multiple comparisons tests.

Fig. 5C is a graph showing comparison of RNP ratios between Cas13a and crRNA in 0.5:1, 1:1, and 1.5:1 ($n = 3$). Bar graphs are shown as mean ± SD, and individual data were plotted as dots. ns, not significant; $^{**}P < 0.01$, $^{****}P < 0.0001$ compared with NC crRNA sample, as assessed by two-way ANOVA with Bonferroni's multiple comparisons tests.

Fig. 5D is a graph showing the optimization of RNP concentration used for liposome encapsulation, ranging from 20 nM to 100 nM ($n = 5$). Bar graphs are shown as mean ± SD, and individual data were plotted as dots. ns, not significant; $^{**}P < 0.01$, $^{****}P < 0.0001$ compared with NC crRNA sample, as assessed by two-way ANOVA with Bonferroni's multiple comparisons tests.

Fig. 6 is a graph showing selection of negative control (NC) crRNA. Four different sequences of NC crRNA were constructed by *in vitro* transcription and compared targeting efficiency with miR-21-5p crRNA. ns, not significant; $^{*}P < 0.05$ compared with miR-21 crRNA samples, as assessed by two-way ANOVA with Bonferroni's multiple comparisons tests.

Fig. 7A - Fig. 7F are representative fluorescence images of the EV miRNA detection assay in EVs from 5 different ovarian cancer cell lines and benign cell line. The miR-21-5p signals (left) and fluorescently labeled EVs (right) from OVCA429 **(A)**, SkOV3 **(B)**, ES-2 **(C)**, CaOV3 **(D)**, OV90 **(E)**, and TiOSE4 **(F)** are shown. Scale bar, 150 μm.

Fig. 8A- Fig. 8C are a series of scatter plots for EVs positive for miR-21-5p (red) in comparison with a negative control group with non-complementary crRNA (blue). EVs were isolated from ovarian cancer cell lines, OV90 (**A**) and OVCAR429 (**B**), as well as benign cell line, TiOSE4 (**C**). Isolated EVs were fused with liposomes containing CRISPR/Cas13a sensing components for miR-21-5p detection. Dotted lines indicate the intensity threshold value to determine the positivity.

Fig. 8D is a graph showing the percentage of positive signals for miR-21-5p from total EV counts for cell line-derived EVs. Bar graphs are shown as mean ± SD from the three independent experiments.

Fig. 8E is a heatmap showing the relative levels of miR-21-5p in EVs from different cell lines measured by RT-qPCR (*top*) and the developed CRISPR/Cas13a detection assay (*bottom*).

Fig. 9 is a graph showing relative abundances of miR-21-5p, as analyzed by RT-qPCR. U6 snRNA levels were served as an internal control. Bar graphs are shown as mean ±SD from the three independent experiments.

Fig. 10A – Fig. 10E is a series of graphs showing the detection of miRNA signature in EVs on antibody-immobilized gold micropattern. The OV90- or TiOSE4-derived EVs were immobilized by IgG isotope control **(A)** and CD63 antibody **(B)**. Representative images of gold micropattern in bright field (*upper*) as well as captured fluorescently labeled EVs (*middle)* and miR-21-5p signal (*bottom*) are shown. Scale bar, 150 μm. The numbers of EVs from OV90 and TiOSE 4 positive for CD63 **(C)**, miR-21-p5 **(D)**, and co-localized signal between EVs and miRNAs **(E)** are shown. ns, not significant; $^{**}P < 0.01$; $^{***}P < 0.001$; $^{****}P < 0.0001$ compared with the OV90 and TiOSE 4, as assessed by two-way ANOVA with

Bonferroni's multiple comparisons tests. Bar graphs are shown as mean ±SD from the three independent experiments.

Fig. 11A is a schematic diagram for detecting miRNA signatures in EpCAM-positive EVs.

Fig. 11B – Fig. 11C are representative images of fluorescently labeled EpCAM-positive EVs (red, *left*) and miRNA signal (green, *right*) in OV90 EVs (**B**) and TiOSE4 EVs (**C**).

Fig. 11D is a graph showing CD63- and EpCAM-positive EV counts from OV90 and TiOSE4 cells. $^{****}P < 0.0001$ compared with the OV90 and TiOSE 4, as assessed by two-way ANOVA with Bonferroni's multiple comparisons tests.

Fig. 11E - Fig. 11F are a series of graphs showing the numbers of miR-21-5p-positive EVs in CD63 (**E**)- or EpCAM-positive EV populations (**F**). $^{***}P < 0.001$; $^{****}P < 0.0001$ compared with the OV90 and TiOSE4, as assessed by two-tailed *t*-test. All bar graphs are shown as mean ± SD.

Fig. 12A is an image of a Western blot showing validation of EV immunoprecipitation with CD63 and EpCAM antibodies, as conducted by western blot analysis.

Fig. 12B - Fig. 12C are a series of graphs showing amplification curves (B) and Ct value (C) of miR-21-5p, as performed by RT-qPCR. ns, not significant compared between EVs from OV90 and TiOSE4 cell lines, as assessed by two-way ANOVA with Bonferroni's multiple comparisons tests. Bar graphs are shown as mean ± SD from the three independent experiments.

Fig. 12D - Fig. 12E are a series of graphs showing melting curve analysis for the PCR products from CD63- or EpCAM-immunoprecipitated EVs (D) and intact EVs (E). Dotted lines indicate the intensity threshold value to determine the Ct value or melting peak.

DETAILED DESCRIPTION OF THE INVENTION

The disclosure provides compositions and methods for amplification-free and extraction-free EV miRNA detection using a CRISPR/Cas13a sensing system. The CRISPR/Cas13a sensing components are encapsulated in liposomes and delivered into EVs through liposome-EV fusion. This allows for accurate quantification of specific miRNA-positive EV counts and detection of target miRNA without complex RNA extraction or amplification. In the Examples provided below, it is shown that miR-21-5p-positive EV counts are in the range of 2~10% in ovarian cancer EVs (OV90, ES-2, OVCA429, SkOV3, CaOV3,), which is significantly higher than the positive EV counts from the benign cells (<0.65%, TIOSE4). The result showed an excellent correlation between bulk analysis with the gold-standard method, RT-qPCR. The Examples also demonstrate multiplexed protein-miRNA analysis in tumor-derived EVs by capturing EpCAM-positive EVs and quantifying miR-21-5p-positive ones in the subpopulation. The methods provided herein may be combined with the immunocapture of target-specific EVs on gold disk arrays to measure miRNA biomarkers in tumor-derived EVs. This EV miRNA sensing system provides a specific miRNA detection method in intact EVs without RNA extraction, allowing for multiplexed single EV analysis for protein and RNA markers.

I. Liposomes

Provided herein are liposomes including components for miRNA biomarker detection. Liposomes are artificially prepared vesicles including a lipid bilayer and may be produced according to standard

methods in the art. For example, a number of commercial preparations of cationic and/or ionizable lipids may be used, such as, e.g., LIPOFECTAMINE™ CRISPRMAX™, LIPOFECTIN® (including DOTMA and DOPE, available from GIBCO/BRL), TRANSIT-TKO™, TRANSMESSENGER™, OLIGOFECTAMINE™, LIPOFECTAMINE™ , SIPORT™, and DHARMAFECT™. In some embodiments, the liposomes described herein are prepared using LIPOFECTAMINE™ CRISPRMAX™. In some embodiments, the liposomes may have a diameter of between about 50 nm to about 200 nm (e.g., about 50 nm to about 100 nm, about 100 nm to about 150 nm, or about 150 nm to about 200 nm).

In some embodiments, lipid nanoparticles may be used instead of liposomes.

1. Cas13a nuclease and crRNA

In some embodiments, the liposome includes a Cas13a nuclease and a crRNA. Cas13a nucleases (CRISPR-class 2, type VI) are RNA-guided RNA nucleases. Exemplary Cas13a nucleases include LwaCas13, LbaCas13, and LbuCas13.

Direct hybridization of a target RNA to crRNA activates the Cas13a's ribonuclease (RNase) activity. The activated Cas13a cleaves crRNA-bounded target RNA (cis-cleavage) and unbounded single-stranded RNA molecules (trans-cleavage). The latter can be used for biosensing applications along with fluorescence-quencher (FQ) probes connected with single-stranded RNA linkers. This approach obviates the reverse transcription step from RNA to cDNA, simplifying the EV miRNA detection.

The crRNA is a polynucleotide sequence having sufficient complementarity with a target nucleic acid sequence (e.g., an miRNA biomarker) to hybridize with the target nucleic acid sequence and direct sequence-specific binding of a Cas13a to the target nucleic acid sequence. A crRNA for Cas13a includes a fixed sequence that forms a stem-loop structure, commonly referred to as a direct repeat or "DR", along with a "Spacer" sequence. Cas13a specifically recognizes and binds to the DR, while the Spacer sequence is complementary to the target nucleic acid. To produce this crRNA via in vitro transcription, DNA oligomers were designed with a DR at the 5' end for binding to Cas13a and a spacer sequence at the 3' end for binding to the target miR-21-5p. In some embodiments, the crRNA binds to a cancer miRNA. Exemplary cancer miRNAs include miR-21-5p (uagcuuaucagacugauguuga, SEQ ID NO: 2). Sequences of exemplary crRNAs are provided in Table 1.

Table 1. Exemplary crRNAs.

crRNA sequence	miRNA target
miR-21-5p crRNA: gauuuagaccaccccaaaaaugaaggggacuaaaacucaacaucag ucugauaagcua (SEQ ID NO: 1)	**miR-21-5p:** uagcuuaucagacugauguuga (SEQ ID NO: 2)

In view of the results described herein, a person of skill in the art can readily design a crRNA to its cognate miRNA.

Direct hybridization of a crRNA to its target (e.g., an miRNA biomarker), which in turn activates the Cas13a's ribonuclease (RNase) activity. The activated Cas13a cleaves crRNA-bounded target RNA (cis-cleavage) and single-stranded RNA molecules (trans-cleavage), such as the single-stranded RNA in the nucleic acid probes described herein.

In some embodiments, the Cas13a nuclease and the crRNA are present at about an equal molar ratio. In some embodiments, the Cas13a nuclease and the crRNA are present at a concentration of between about 50 nM to about 150 nM (e.g., about 50 nM to about 60 nM, about 60 nM to about 70 nM, about 70 nM to about 80 nM, about 80 nM to about 90 nM, about 90 nM to about 100 nM, about 100 nM to about 110 nM, about 110 nM to about 120 nM, about 120 nM to about 130 nM, about 130 nM to about 140 nM, or about 140 nM to about 150 nM). In some embodiments, the Cas13a nuclease and the crRNA are present at a concentration of about 100 nM.

2. Nucleic acid probe

The nucleic acid probes include a detectable label, a nucleic acid linker, and a quencher. In some embodiments, a detectable label may be configured at the 5' or 3' end of the nucleic acid probe. In some embodiments, the nucleic acid probe includes 5' [detectable label]-[nucleic acid linker]-[quencher] 3'. In one working example, the nucleic acid probe includes the following structure: 5' FAM-TAuuGC- IABkFQ 3', where FAM is the detectable label, TAuuGC is the nucleic acid linker, and IABkFQ is the quencher.

In some embodiments, the nucleic acid probe includes 5' [quencher]-[nucleic acid linker]-[detectable label] 3'. In some embodiments, the nucleic acid probe includes the following structure: 5' IABkFQ -TAuuGC- FAM 3'.

a) Detectable label

The detectable label is a molecule or complex useful for detection of a desired target molecule (e.g., a nucleic acid). Detectable labels emit an optical signal that is readily detected by methods known in the art including fluorescence, chemiluminescence, absorbance and the like. Detectable labels include fluorophores, radioisotopes, chromophores, enzymes, dyes, ligands such as biotin, avidin, streptavidin and haptens, quantum dots, and the like. In some embodiments, the detectable label is a fluorophore. Exemplary fluorophores include fluorescein amidite (FAM), fluorescein isothiocyanate (FITC), rhodamine, tetramethylrhodamine isothiocyanate (TRITC), 4',6-diamidino-2-phenylindole (DAPI), coumarin, cyanine, xanthene, naphthalene, oxadiazole, anthracene, pyrene, oxazine, acridine, arylmethine, tetrapyrroles, Alexa Fluor compounds, and BODIPY, or derivatives or conjugates thereof. In some embodiments, the fluorophore is fluorescein amidite (FAM). The fluorescence signal from a fluorescent detectable label on the nucleic acid probe may be measured using an upright fluorescent microscope.

b) Nucleic acid linker

In some embodiments, the nucleic acid linker includes RNA nucleotides. In some embodiments, the nucleic acid linker includes both RNA and DNA nucleotides. In some embodiments, the nucleic acid linker includes 5' DNA-RNA-DNA 3'. In some embodiments, the nucleic acid linker includes the sequence of TAuuGC (SEQ ID NO: 3). The nucleic acid linker triggers fluorescence signals through cleavage by Cas13a's RNase activity. In this context, for preventing non-specific cleavage, the RNA sequence typically prevents non-specific cleavage. Longer RNA sequences typically correlate with increased non-specific cleavage. Therefore, it is advantageous to include two RNA sequences within the length Cas13a can recognize (typically 10, 9, 8, 7, 6, or 5 nucleotides, preferably 6 nucleotides).

c) Quencher

The quencher is a molecule that prevents a detectable label from emitting a detectable optical signal. In some embodiments, a quencher prevents a fluorophore from fluorescing. In some embodiments, a quencher may only prevent the fluorophore from fluorescing if the quencher is in close physical proximity to the fluorophore, as is well understood in the art. Exemplary quenchers include 3' IOWA BLACK® FQ (IABkFQ), BLACK HOLE QUENCHER®-1, BLACK HOLE QUENCHER®-2, Dabcyl, and BLACK HOLE QUENCHER®-3. In some embodiments, the quencher is IABkFQ. In some embodiments, the nucleic acid probe includes one or more quenchers.

II. EV-liposome fusion

Also provided herein are fusions between an extracellular vesicle (EV) and a liposome described herein. In the EV-liposome fusion, the two initially distinct lipid bilayers merge their hydrophobic cores, resulting in one interconnected structure.

CRISPR sensing components (Leptotrichia wadei/LwaCas13a, crRNA, and FQ probes) incorporated in liposomes are delivered to EVs through EV-liposome fusion. EV-liposome fusion is an efficient way to deliver sensing materials inside individual EVs, allowing for the detection of target miRNA without complex RNA extraction or amplification.

EVs are nano-sized secretory particles originating from the cellular endosomal trafficking system. EVs contain molecular cargo, including common and cell-specific proteins, nucleic acids, and lipids, reflecting the physiological characteristics of cells of origin. The EVs include a lipid bilayer membrane enclosing contents of the internal cavity. An EV can include, but is not limited to, an ectosome, a microvesicle, a microparticle, an exosome, an oncosome, an apoptotic body, a liposome, a vacuole, a lysosome, a transport vesicle, a secretory vesicle, a gas vesicle, a matrix vesicle, or a multivesicular body. In some embodiments, the EV is between about 50 nm to about 250 nm (e.g., about 50 nm to about 100 nm, about 100 nm to about 150 nm, about 150 nm to about 200 nm, or about 200 nm to about 250 nm). In some embodiments, the EV is a tumor-derived EV, which is an EV that is released from a tumor cell.

In some embodiments, the EVs include a miRNA biomarker (e.g., a cancer biomarker). miRNAs are small non-coding RNAs involved in post-transcriptional gene regulation by inhibiting translation and cleavage of their target RNA transcripts. miRNAs are involved in disease initiation and progression. Thus, up- or down-regulation of specific miRNA can be used as a diagnostic marker for cancers, cardiovascular diseases, lung diseases, and neurodegenerative diseases, among many others. In addition, EV miRNAs play essential roles in cell-to-cell communications. Therefore, accurate, quantitative measurements of EV miRNAs become critical for the clinical translation of the diagnostic biomarkers and a better understanding of EV-medicated biological processes.

In some embodiments, fusion of the EV and liposome is promoted by electrostatic interactions. In some embodiments, the fusion rate of the EV and liposomes is at least 80% (e.g., at least 85%, at least 90%, at least 95%, or at least 99%).

In some embodiments, the EV-liposome fusion is between about 300 nm to about 500 nm (e.g., about 300 nm to about 350 nm, about 350 nm to about 400 nm, about 400 nm to about 450 nm, or about 450 nm to about 500 nm).

III. Array

Also provided herein are arrays. An array is a substrate including a plurality of nanostructures with one or more immobilized capture moieties fixed on or adjacent to the nanostructures.

In some embodiments, the array is a gold microdisk array. Microdisks are micron-sized, e.g., between about 1 μm to about 50 μm (e.g., about 1 μm to about 5 μm, about 5 μm to about 10 μm, about 10 μm to about 15 μm, about 15 μm to about 20 μm, about 20 μm to about 25 μm, about 25 μm to about 30 μm, about 30 μm to about 35 μm, about 35 μm to about 40 μm, about 40 μm to about 45 μm, or about 45 μm to about 50 μm, preferably about 1 μm to about 10 μm). In some embodiments, the array is a gold nanodisk array. Nanodisks are sub-micron sized, e.g., between about 50 nm to about 1 μm (e.g., about 50 nm to about 100 nm, about 100 nm to about 200 nm, about 200 nm to about 300 nm, about 300 nm to about 400 nm, about 400 nm to about 500 nm, about 500 nm to about 600 nm, about 600 nm to about 700 nm, about 700 nm to about 800 nm, about 800 nm to about 900 nm, or about 900 nm to about 1 μm). In some embodiments, the nanodisk is 500 nm. The nanodisks are designed to capture single EV on each disk, while microdisks may capture multiple EVs on each disk. Nanodisks have advantages for specific capture of tumor-derived EVs and their quantification.

In some embodiments, the immobilized capture moieties on the array are arranged in a grid pattern. The gold microdisk and nanodisk arrays immobilize capture antibodies using a direct physisorption method with ultralow nonspecific binding of EVs to the gold surface. In some embodiments, the gold disk arrays capture marker-specific EVs on the designed binding areas in a grid pattern. The pattern reduces the probability of false-positive signals from non-specifically bound EVs (i.e., improved specificity) and simplifies image analysis.

The immobilized capture moiety may be any molecule with the ability to bind to a target (e.g., a tumor-derived EV). Suitable capture moieties include, but are not limited to antibodies or antigen-binding fragments thereof. In some embodiments, the immobilized capture moiety is an anti-EpCAM antibody. EpCAM is a cancer marker that is over expressed in ovarian cancer. In some embodiments, the immobilized capture moiety is an antibody that binds a protein over-expressed in solid tumors (e.g., EGFR, MUC1, MUC16, CD24, or HER2). In some embodiments, the immobilized capture moiety is an antibody that binds a protein associated with drug resistance (for example, chemotherapy resistance) (e.g., poly-glycoprotein or survivin).

In some embodiments, the array includes an immobilized capture moiety and a tumor-derived EV. In some embodiments, between about 10^7 to about 10^9 EVs are applied to the array. In some embodiments, about 10^8 EVs are applied to the array. In some embodiments, the array includes an immobilized capture moiety and an EV-liposome fusion described herein (e.g., a tumor-derived EV-liposome fusion).

III. Methods

Also provided herein are methods for detecting an miRNA biomarker in a tumor-derived EV. The detection methods provided herein are amplification-free and extraction-free using a CRISPR/Cas13a sensing system. The CRISPR/Cas13a sensing components are encapsulated in liposomes and delivered into EVs through liposome-EV fusion. This allows for EV miRNA detection without the need for sequential steps of EV lysis, RNA extraction, and reverse transcription, which is commonly required in conventional

EV RNA analysis. This method allows EV RNA detection in intact EVs and reports quantitative positive EV counts for specific miRNA targets.

EVs present in a patient plasma sample are heterogenous with different subpopulations from various cellular origins. The current EV RNA analysis methods that involve EV lysis lose the information and prevent accurate quantification within certain subpopulations. The methods and compositions provided herein enable quantifying EVs containing target RNA and multiplexed EV protein and RNA analysis.

In some embodiments, the method includes detecting an miRNA biomarker in a tumor-derived EV, the method including detecting the miRNA biomarker in any EV-liposome fusion described herein. The detection assay may be carried out in solution, e.g., the liposomes may be incubated with the EVs in solution, then the mixture may be mounted on a glass slide and analyzed using microscopy.

In some embodiments, the miRNA detection assay may be carried out on an array described herein. Detection of the miRNA in the EV-liposome fusions on the gold arrays allows for capture of only the tumor-derived EVs, which is advantageous because the tumor-derived EV portion is small compared to all EVs presented in a plasma sample.

In some embodiments, the method includes the steps of: (a) providing an array described herein including a plurality of immobilized capture moieties that specifically bind a tumor-derived EV; (b) binding the tumor-derived EVs to the array; (c) incubating the bound tumor-derived EVs with any liposome provided herein; and (d) detecting the miRNA biomarker.

In some embodiments, the method includes the steps of: (a) providing an array described herein including a plurality of immobilized capture moieties that specifically bind a tumor-derived EV; (b) binding an EV-liposome fusion described herein; and (c) detecting the miRNA biomarker.

In some embodiments, the presence or level of an miRNA biomarker in a sample from a patient identifies the patient as having a disorder (e.g., a cancer). In some embodiments, the absence or level of an miRNA biomarker in a sample from a patient identifies the patient as not having a disorder (e.g., a cancer).

In some embodiments, the methods provided herein detect miR-21-5p in EVs from ovarian cancer. miR-21-5p is over-expressed in ovarian cancer tissues, cells, and their EVs. As described in the Examples below, 2~10% of EVs from ovarian cancer cell lines showed positive signals for miR-21-5p, which correlated well with the bulk analysis with the gold-standard method.

In some embodiments, the method further includes detecting one or more proteins on the EV-liposome fusion by immunolabeling. In some embodiments, the one or more proteins are over-expressed in solid tumors (e.g., EGFR, MUC1, MUC16, CD24, or HER2). In some embodiments, the one or more proteins are associated with drug resistance, such as chemotherapy resistance (e.g., poly-glycoprotein or survivin).

In some embodiments, the methods can be combined with the immunocapture of target-specific EVs on gold disk arrays to measure miR-21-5p for EpCAM-positive, tumor-derived EVs. These demonstrate the specific miRNA detection in intact EVs without RNA extraction and the possibility of multiplexed single EV analysis for protein and miRNA markers.

EXAMPLES

Table of Contents

Example 1	Materials and methods
Example 2	CRISPR/Cas13a-triggered EV miRNA detection assay
Example 3	Purification of LwaCas13a
Example 4	Optimization of EV miRNA detection assay
Example 5	miR-21-5p detection in EV from ovarian cancer cell lines
Example 6	Detection of miR-21-5p in cancer marker expressing EVs
Example 7	Detection of surface proteins by immunolabeling

Example 1. Materials and methods

Bacterial expression and purification of LwaCas13a

LwaCas13a was purified by bacterial expression followed by Ni-NTA purification (Fig. 2A). The LwaCas13a-expression plasmid, pC013 - Twinstrep-SUMO-huLwCas13a was a gift from Feng Zhang (Addgene plasmid # 90097; http://n2t.net/addgene:90097; RRID:Addgene_90097) (Gootenberg et al. *Science* **2017,** *356*, 438-442). The plasmid was transformed into the bacterial protein expression *E.coli* strain, Rosetta 2(DE3) pLysS (Millipore Sigma) by heat shock. The single colony was inoculated and then cultured in Terrific buffer at 37°C until the value of optical density at 600 nm reached 4. Next, the transformed cells were incubated at 21°C for 16 hr after 0.5 mM IPTG induction. The cells were harvested and stored at -80°C until protein purification. For purification of LwaCas13a, the cells were lysed in bacterial cell lysis buffer (50 mM NaH_2PO_4, 500 mM NaCl, 1 mg/mL lysozyme, and protease inhibitor) at 4°C for 30 min and followed by sonication for 1 hr in cold condition. The lysed bacterial proteins were collected by centrifugation with 10,000 X G for 1 hr at 4°C. While collecting lysate, the NI-NTA column was prepared. The Ni-NTA resin (ThermoFisher Scientific) was packed into the glass Econo-Column (BioRad) and washed twice with excess Ni-NTA wash buffer (50 mM NaH_2PO_4, 500 mM NaCl, 0.2% Triton X-100, 20 mM imidazole, and protease inhibitor). The lysate was introduced into the NI-NTA column and incubated at 4°C for 2 hr with gentle shaking, followed by draining the flow-through and washing the Ni-NTA resin with Ni-NTA wash buffer. The resin-bounded proteins were eluted with Ni-NTA elution buffer (50 mM NaH_2PO_4, 500 mM NaCl, and 250 mM imidazole). The eluate was concentrated by centrifugal filter (Millipore Sigma, 100K MWCO) with the addition of SUMO cleavage buffer (30 mM Tris-HCl (pH 8.0), 500 mM NaCl, and 1 mM DTT). Next, the filtrate was treated with SUMO protease (ThermoFisher Scientific) that was tagged with polyhistidine at 5 'terminus at 4°C for overnight with gentle shaking. The new Ni-NTA column was prepared and pre-washed with SUMO-NI-NTA wash buffer (30 mM Tris-HCl (pH 8.0), 500 mM NaCl, 20 mM imidazole, and 1 mM DTT). The SUMO protease-cleaved product was introduced into the NI-NTA column to remove the SUMO protease and incubated at 4°C for 2 hr with gentle shaking. The flow-through was collected and concentrated with the centrifugal filter (100K MWCO) with the addition of storage buffer (50 mM Tris-HCl (pH 7.5), 600 mM NaCl, and 2 mM DTT). The protease inhibitor and 5% glycerol were added to the filtrate and stored until used at -80°C.

crRNA generation

The crRNAs for miRNA detection were generated by *in vitro* transcription (Fig. 2B). Briefly, DNA templates, which are composed of T7 promoter sequence and their complementary sequence, were annealed by controlling temperature from 95°C to room temperature in annealing buffer (20 mM Tris-HCl (pH 8.0), 50 mM NaCl, and 1 mM EDTA). *In vitro* transcription was performed by manufacturer's instruction (Promega) at 37 for 30 min, followed by DNaseI treatment for eliminating template DNAs. The transcribed RNA was then isolated by ethanol precipitation and confirmed the concentration by Qubit RNA assay kit (ThermoFisher Scientific) and quality by 15% denaturing PAGE, followed by SYBR gold staining (ThermoFisher Scientific).

In vitro LwaCas13a-mediated miRNA detection assay

The LwasCas13a reaction mixture was prepared with 100 nM LwaCas13a, 100 nM NC or miR-21-5p crRNA, 20U RNase inhibitor (Promega), 40 nM 6-carboxyfluorescein (FAM)-tagged quencher reporter, and indicated concentration of NC small RNA or mature miR-21-5p in 1X Cas13a reaction buffer (40 mM Tris-HCl (pH 7.5), 60 mM NaCl, and 6 mM $MgCl_2$) and incubated at 37°C for 30 min. The fluorescent intensities were measured by a multi-plate reader (Tecan).

Cell culture

The human carcinoma cell lines, including OVCA429, SkOV3, OV90, CaOV3, and ES-2 cells, were purchased from American Type Culture Collection (ATCC). TIOSE4 was obtained from transfection of hTERT into NOSE cells maintained in 1:1 Media 199:MCDB 105 with gentamicin (25 µg/mL), 15% heat-inactivated serum, and G418 (500 µg/mL) (Zorn et al. *Clin Cancer Res* **2003,** *9*, 4811-4818). OVCA429, SkOV3, OV90, and TiOSE4 cells were maintained in RPMI-1640 (Hyclone). ES-2 and CaOV3 cells were cultured in McCoy's 5A (Gibco) and DMEM (Hyclone), respectively. All complete media were supplemented with 10% fetal bovine serum (FBS, ThermoFisher Scientific), 100 U/mL penicillin, and 100 µg/mL streptomycin (Cellgro) at 37 °C in 5% CO_2. All cell lines were tested and confirmed that they were free of mycoplasma, as conducted with Universal Mycoplasma Detection Kit (ATCC).

EV isolation and fluorescence labeling

For EV collection from different cell lines, the cells were cultured in a complete medium until they were 80-90% confluent. After brief PBS washing for 2 times, the cells were incubated with the basal medium for each cell line supplemented with 1% exosome-depleted FBS (ThermoFisher Scientific), 100 U/mL penicillin, and 100 µg/mL streptomycin for 48 h. The EV isolation was conducted by size exclusion chromatography (SEC) as the previous description (Min et al. *Adv Biosyst* **2020,** *4*, e2000003, Van Deun et al. *Adv Biosyst* **2020,** *4*, e1900310). Briefly, the conditioned medium was collected with a 40 µm-sized cell strainer (Corning) and spun at 300 x g for 5 min to remove the cell debris. The supernatant was filtered through a 0.8 µm membrane filter (Millipore Sigma) and spun at 3,500 x g for 30 min at 4°C by using Centricon Plus-70 Centrifugal Filter (MWCO = 10 kDa, Millipore Sigma). The concentrates were loaded onto the top of the SEC column, which was packed with 10 mL of Sepharose CL-4B (GE Healthcare) in a 10 mL syringe (BD Biosciences). The fractions of 4 and 5 of 1 mL were collected and concentrated with the Amicon Ultra-2 Centrifugal Filter (MWCO = 10 kDa, Millipore Sigma) at 3,500 x g

for 30 min at 4°C. The protease and phosphatase inhibitor cocktail (ThermoFisher Scientific) was added and stored until use at -80°C.

EVs were labeled with AF647 dye, as previously reported (Ferguson et al. *Sci Adv* **2022,** *8*, eabm3453). Briefly, 27.5 mM of Azido-dPEG®$_{12}$-TFP ester (Quanta Biodesign) and 25 mM of AFDye 647 DBCO (Click Chemistry Tools) were prepared in anhydrous DMSO (Millipore Sigma) and mixed in an equal volume followed by incubation at RT for 2 hr. Next, 3 μL of EVs in PBS, 2 μL of 100 mM sodium bicarbonate (Millipore Sigma), and 0.2 μL of TFP-AF647 were mixed and incubate at RT for 1 hr. The labeled EVs were diluted with PBS in an appropriate concentration before use.

EV-liposome fusion-based miRNA detection assay in solution

The liposome complex was prepared with Lipofectamine Crispmax Cas9 Transfection reagent (ThermoFisher Scientific) by brief modification of the manufacturer's instruction. Briefly, the complex A, including 100 nM LwaCas13a, 100 nM NC or miR-21-5p crRNA, 20U RNase inhibitor, and 40 nM FAM-tagged quencher reporter, was prepared in 1X Cas13a reaction buffer. Additionally, complex B was prepared by gently mixing transfection reagent with 1X Cas13a reaction buffer in an equal volume of complex A. The complex A and B were gently mixed and incubated at RT for 15 min. Next, the AF647-labeled EVs diluted in 1X Cas13a buffer were introduced into the complex and incubated at 37°C for 30 min. After incubation, the fusion complex was mounted on the TPFE-printed glass slide (Electron Microscopy Sciences) and analyzed using an upright fluorescent microscope (Zeiss).

EV-liposome fusion-based miRNA detection assay on gold-micropattern

Antibody immobilization on gold microdisk arrays was conducted, as described previously. Briefly, CD63 (Ancell) or EpCAM (Invitrogen) antibodies, respectively diluted by 1:100 or 1:20 in 10 mM phosphate buffer, were treated on the surface for 1 hr. After washing out the non-bounded antibodies with PBS, 10% BSA in PBS was treated for blocking. Next, the AF647-labeled EVs derived from OV90 or TiOSE4 were incubated for 1 hr. The complex for the EV-miRNA detection system was then introduced and incubated at 37°C for 1 hr. After washing with PBST, the fluorescent signal was obtained by an upright fluorescent microscope (Zeiss).

Western blotting

EVs derived from ovarian cancer lines were lysed in LIPA lysis buffer (Cell Signaling Technology) containing protease inhibitor (Roche). Western blot analysis was performed as described previously. The nitrocellulose membrane blots were probed with anti-CD9 (1:500 dilution, BD Biosciences), anti-CD63 (1:500 dilution, Ancell), and anti-CD81 (1:500 dilution, Santa Cruz Biotechnology). The chemiluminescence signal was detected with an Azure 280 imaging system (Azure Biosystems).

Quantitative RT-PCR analysis

Small RNAs from 6 different ovarian cancer cell EVs were analyzed by RT-qPCR to evaluate the miRNA expression levels as described previously. Briefly, small RNAs were reverse transcribed and polyadenylated simultaneously with oligo(dT)-linked adaptor oligomer (see Table 2) at sequential 37°C for 1 hr, 42°C for 30min and 70°C for 10 min. The quantitative PCR was performed with cDNAs, gene-

specific forward and universal reverse primer set, and 2X SsoAdvanced Universal SYBR Green Supermix (Biorad) by CFX Opus Real-Time PCR Systems (Biorad). The relative miRNA expression was calculated by the $2^{-\Delta\Delta Ct}$ method. U6 snRNA served as an internal control. Oligonucleotides used in RT-qPCR are provided in Table 2.

Table 2. Sequences of oligomers. V = A, C, or G; N = A, C, G, or T. Lower case letters denote RNA.

Name	Sequence (5' to 3')
miR-21-5p-F	TAGCTTATCAGACTGATGTTGA (SEQ ID NO: 4)
U6 snRNA-F	CAAATTCGTGAAGCGTTCCA (SEQ ID NO: 5)
universal-R	AGGCAGTGGTATCAACGCAGA (SEQ ID NO: 6)
miR-RT-adaptor	AGGCAGTGGTATCAACGCAGAGTACTTTTTTTTTTTTTTTTTTTTTTTTTTTTTTVN (SEQ ID NO: 7)
T7-univeral upper	TAATACGACTCACTATAG (SEQ ID NO: 8)
T7-bottom NC-1	TTGTACTACACAAAGTACTGGTTTTAGTCCCCTTCATTTTTGGGGTGGTCTAAATCTATAGTGAGTCGTATTA (SEQ ID NO: 9)
T7-bottom NC-2	TTGTACTACACAAAAGTACTGGTTTTAGTCCCCTTCATTTTTGGGGTGGTCTAAATCTATAGTGAGTCGTATTA (SEQ ID NO: 10)
T7-bottom NC-3	CCCCCCCCCCCCCCCCCCCCCGTTTTAGTCCCCTTCATTTTTGGGGTGGTCTAAATCTATAGTGAGTCGTATTA (SEQ ID NO: 11)
T7-bottom NC-4	AAAAAAAAAAAAAAAAAAAAAGTTTTAGTCCCCTTCATTTTTGGGGTGGTCTAAATCTATAGTGAGTCGTATTA (SEQ ID NO: 12)
T7-bottom miR-21-5p	TAGCTTATCAGACTGATGTTGAGTTTTAGTCCCCTTCATTTTTGGGGTGGTCTAAATCTATAGTGAGTCGTATTA (SEQ ID NO: 13)
miR-21-5p	uagcuuaucagacugauguuga (SEQ ID NO: 2)
NC-1	uuguacuacacaaaguacug (SEQ ID NO: 15)
Poly U probe	FAM-uuuuu-Quencher
DRD probe	FAM-TAuuGC-Quencher
Double quencher probe	FAM-uuuuuuuu-Quencher-uu-Quencher

Example 2. CRISPR/Cas13a-triggered EV miRNA detection assay.

Existing EV miRNA detection methods start from RNA extraction from EV lysates. This prevents analysis of miRNA levels in intact EVs for multiplexed analysis. To address the limitation, the inventors developed the Cas13a-mediated miRNA detection system for intact EVs without EV lysis. Specifically, liposomes were prepared containing LwaCas13a-crRNA ribonucleoproteins (RNPs) and fluorophore-quencher (FQ) probes and fused with EVs by electrostatic interactions (**Fig. 1A**). The hybridization of target miRNAs with complementary sequence-harboring crRNA activates LwaCas13a. The activated LwaCas13a cleaves RNA sequences in the FQ probe, generating fluorescence signals inside liposome-fused EVs detected by a conventional fluorescence microscope. This method allows for detecting specific miRNAs in intact EVs without reverse transcription or PCR-based gene amplification.

The detection system was first tested using EVs from the ES2 ovarian cancer cell line. EVs were isolated by size-exclusion chromatography. The isolated EVs showed the characteristic EV size distribution of 50-250 nm in diameter measured by nanoparticle tracking analysis (**Fig. 1B**, *left*), which was further validated with the presence of the common EV markers, such as CD9, CD63, and CD81 by western blotting (**Fig. 2**). Next, liposomes were prepared containing ribonucleoprotein (RNP) complexes (LwaCas13a and miRNA-targeting crRNAs) and FQ probes using a cationic transfection reagent, Lipofectamine CRISPRMAX, which was known as the best nanocarrier for delivering Cas9 RNP complexes into target cells. The liposomes showed a similar size distribution to EVs in the range of 50-200 nm (**Fig. 1B**, *middle*). Liposome-EV fusion formed fusosomes with enlarged size distribution (**Fig. 1B**, *right*). The liposome-EV fusion efficiency was calculated by measuring the co-localization of fluorescently labeled EVs and fluorescence oligomers (**Fig. 1C**) or immunoglobulin inside liposomes (**Fig. 3**). The results show an efficient fusion rate of >80% signal co-localization after 30 min incubation.

Example 3. Purification of LwaCas13a.

LwaCas13a was purified from bacterial expression with a LwaCas13a-expression plasmid, followed by Ni-NTA (nickel-nitrilotriacetic acid) purification. Briefly, the plasmid, composed of 6XHis-Twinstrep-SUMO-LwaCas13a, was transformed into the Rosetta 2(DE3) pLysS *E.coli* strain and induced by isopropylthio-β-galactoside (IPTG) treatment. Cells were lysed and purified by 1st Ni-NTA purification to capture the N-terminal polyhistidine residue. The eluate was then treated with polyhistidine-tagged SUMO protease to cleave the internal SUMO cleavage sequence, upstream of LwaCas13a sequence. Finally, the N-terminal cleaved residue and SUMO protease were removed by 2nd Ni-NTA purification, and unbounded LwaCas13a was collected. SDS-PAGE analysis by silver staining shows clear LwaCas13a product near 150 kDa size with high integrity (**Fig. 4A**; please see Materials and Methods for details). crRNA for miR-21-5p and corresponding negative control was synthesized by *in vitro* transcription, followed by DNase treatment and purification (**Fig. 4B**; please see Materials and Methods for details). The final product corresponding to crRNAs for miR-21-5p (SEQ ID NO: 1) and negative control were generated and clearly purified, as performed denaturing polyacrylamide gel electrophoresis (PAGE) and SYBR gold gel staining. The trans-cleavage activity of LwaCas13a and the cleavage specificity *in vitro* was then investigated. In titrating miR-21-5p concentrations, it showed a corresponding decrease in fluorescence signals of FQ-probes generated by the trans-cleavage of RNA linkers by activated LwaCas13a (**Fig. 4C**), while no signal changes were measured against non-complementary miRNA targets (**Fig. 4D**). Additionally, the activity and specificity of the detection system in EVs from Gli261 miR-21 knock-out and wild-type cell lines was tested. EVs were fluorescently labeled by AF647 (shown in red) and their co-localization with green fluorescence signals of FQ probes after liposome-EV fusion was analyzed (**Fig. 4E**). The presence of miR-21-5p in EVs activated LwaCas13a, which cleaved FQ probes, generating green fluorescence signals. The analysis showed green fluorescence signals were co-localized EVs 'signals well, and about 2.4% of EVs from wild-type Gli261 cell lines were positive for miR-21-5p. In contrast, the negative control EVs from the miR-21 knock-out Gli261 cell line showed a negligible background signal in less than 0.1% ($n = 4$, $p < 0.05$, Mann Whitney test; **Fig. 4F**).

Example 4. Optimization of EV miRNA detection assay.

Sensing components in liposomes (RNPs, FQ probes) for Cas13a-based EV miRNA detection were then optimized (**Fig. 5A**). EVs from ES2 ovarian cancer cell line were used for testing. As a negative control, liposomes with non-complementary crRNA to measure background signals were used as a negative control (**Fig. 6**). Three different cleavage sequences of FQ probes were tested: 1) fluorescein amidite (FAM)-rUrUrUrUrU-Quencher, 2) FAM-TArUrUGC-Quencher, and 3) FAM-rUrUrUrUrUrUrUrU-Quencher-rUrU-Quencher. The first two probes were from previous work with the difference of RNA linker vs. DNA-RNA-DNA linker (Gootenberg et al. *Science* **2018,** *360*, 439-444). The third probe has double quenchers to test if this configuration could further decrease the background signal. The test result showed that only the probe designed with DNA-RNA-DNA linkers between FAM and quencher showed a significant difference between miR-21-5p and control samples ($p < 0.0001$, **Fig. 5B**). The double quencher probe indeed reduced the background signals from the control sample, but the miR-21-positive signal also decreased, resulting in no significant difference from the control sample.

Next, different RNP ratios between LwaCas13a and crRNAs were tested, and the equal molar ratio showed the most significant difference between miR-21-5p and control samples (**Fig. 5C**). Furthermore, RNP concentrations of 50 nM ($p < 0.01$) and 100 nM ($p < 0.0001$) showed significant differences (**Fig. 5D**). Taken together, the optimal condition for EV miRNA detection assay with FQ probes was determined to be the DNA-RNA-DNA linker (TArUrUGC) and an equal amount of LwaCas13a and crRNA in 100 nM concentration. The optimized condition was then applied to the following experiments.

Example 5. miR-21-5p detection in EV from ovarian cancer cell lines.

The CRISPR/Cas13a system was applied to detect miR-21-5p in EVs from five different ovarian cancer cell lines (OVCA429, SkOV3, ES-2, CaOV3, and OV90) and one benign cell line (TIOSE4). Isolated EVs from the cell lines were labeled, followed by fluorescent labeling using AF647 dye (please see Methods for the detailed protocol), and then CRISPR liposomes were applied. We then measured FAM fluorescence signals inside EVs (defined by the co-localization with EV signals in the AF647 channel) produced from Cas13a trans-cleavage in the presence of miR-21-5p (please see **Fig. 7A - Fig. 7F** for fluorescence images). Another liposome with non-complementary crRNA was used as a negative control. **Fig. 8A - Fig. 8C** show scatter plots of EV and miR-21-5p signals from cell-line derived EVs with high (OV90), moderate (OVCAR429), and low (TIOSE4) levels of miR-21-5p. The cut-off intensities were set based on the negative control signals with non-complementary crRNA, which is mean + 3 times of standard deviation. miR-21-5p-positive EV percentage over the total number of EVs was counted. The result showed that miR-21-5p-positive EV counts are in the range of 2~10% in ovarian cancer EVs (OV90, 10.22%; ES-2, 6.37%; OVCA429, 4.48%; SkOV3, 2.66%; CaOV3, 2.53%), which is significantly higher than the positive EV counts from the benign cells (TIOSE4, 0.08%, **Fig. 8D**).

To validate the result, the relative abundance of miR-21-5p was measured using the gold standard reverse transcription-quantitative polymerase chain reaction (RT-qPCR). Small RNAs from different cell line-derived EV lysates were reverse transcribed, and the cDNAs were amplified with a miR-21-5p-specific primer pair to measure the relative abundances of miR-21-5p (**Fig. 9**). The miR-21-5p signals measured by the CRISPR/Cas13 system showed a good correlation with the RT-qPCT result

(Pearson correlation coefficient, $r = 0.872$, $p < 0.05$, **Fig. 8E**). Taken together, the CRISPR system for miRNA detection in EVs indicated the potential for direct detection of miRNAs in intact EVs without extra RNA isolation, reverse transcription, and target amplification.

Example 6. Detection of miR-21-5p in cancer marker expressing EVs.

Fig. 11A shows the multiplexed detection strategy for tumor-derived EVs and a miRNA marker in the subpopulation. Gold microdisk arrays were made to immobilize capture antibodies using a direct physisorption method that showed ultralow nonspecific binding of EVs to the gold surface. The gold disk arrays were designed to capture marker-specific EVs on the designed binding areas in a grid pattern. The pattern reduces the probability of false-positive signals from non-specifically bound EVs (i.e., improved specificity) and simplifies image analysis. Antibodies against CD63, a generic EV marker, and EpCAM, a cancer marker showing over expressions in ovarian cancer, were used. Fluorescently labeled EVs (~10^8 EVs) from OV90 and TIOSE4 cell lines were applied on the antibody-coated gold disk arrays, followed by CRISPR-liposome fusion for miR-21-5p detection in captured EVs. The result showed that only EVs from the OV90 ovarian cancer cell line were captured by anti-EpCAM-coated gold disk arrays, while the binding of EVs from the TIOSE4 benign cell line was negligible, similar to the binding to the IgG isotype control (**Fig. 11B - Fig. 11D**). For anti-CD63-coated gold arrays, EVs from both cell lines were captured (positive control, **Fig. 11D**). For CD63- and EpCAM-positive EVs, OV90 EVs showed a significantly higher positivity for miR-21-5p than TiOSE4 EVs (**Fig. 11E and Fig. 11F**). In conventional processes by immunoprecipitation with anti-CD63 or anti-EpCAM followed RT-qPCR, however, neither miR-21-5p nor significant differences were detected between OV90 and TiOSE4 EVs even if 20-times higher EV amounts were used (~2×10^9 EVs; **Fig. 12A - Fig. 12E**). These results indicate that the developed assay showed at least 20-fold higher sensitivity than the conventional RNA immunoprecipitation assay for detecting miRNAs in tumor-derived EVs. Collectively, the significantly higher expressions of EpCAM and miR-21-5p in ovarian cancer-derived EVs can be used to further improve the specificity in detecting tumor-derived EVs.

Example 7. Detection of surface proteins by immunolabeling.

In a working example, after EV capture and liposome fusion, additional antibodies targeting different surface proteins on EVs are applied to the captured EVs. The antibodies are either directly conjugated with fluorophores or labeled by fluorophore-conjugated secondary antibodies. The labeled EVs are imaged under a fluorescence microscope having multiple fluorescence channels. The number of channels is typically 4 to 6, while additional channels can be assigned according to standard techniques.

Markers detected by additional antibodies may include markers known to be overexpressed in cancers (e.g., MUC1, EGFR, HER2, Trop2, CD24, WNT2, GPC1). The co-existence of multiple cancer biomarkers increases the specificity of detecting tumor-derived EVs.

Markers detected by additional antibodies may include markers associated with certain targeted drugs (e.g., PD-L1, HER2, folic receptor alpha, MUC16). The co-existence of markers associated with certain targeted drugs within captured tumor-derived EVs indicates the potential efficacy of these targeted drugs.

Markers detected by additional antibodies may include markers associated with chemotherapeutic drug resistance (e.g., poly-glycoprotein, survivin, Cyclin D1, tubulin). The co-existence of drug-resistance markers indicates the potential risk of drug resistance.

OTHER EMBODIMENTS

While the invention has been described in connection with specific embodiments thereof, it will be understood that it is capable of further modifications and this application is intended to cover any variations, uses, or adaptations of the invention following, in general, the principles of the invention and including such departures from the present disclosure come within known or customary practice within the art to which the invention pertains and may be applied to the essential features hereinbefore set forth. All publications, patents, and patent applications are herein incorporated by reference in their entirety to the same extent as if each individual publication, patent, or patent application was specifically and individually indicated to be incorporated by reference in its entirety.

Some embodiments of the technology described herein can be defined according to any of the following numbered embodiments:

E1. A liposome comprising a Cas13a nuclease, a crRNA, and a nucleic acid probe, wherein the nucleic acid probe comprises a detectable label, a nucleic acid linker, and a quencher.

E2. An extracellular vesicle-liposome (EV-liposome) fusion comprising a Cas13a nuclease, a crRNA, and a nucleic acid probe, wherein the nucleic acid probe comprises a detectable label, a nucleic acid linker, and a quencher.

E3. The liposome of E1 or the EV-liposome fusion of E2, wherein the EV is a tumor-derived EV.

E4. The liposome or EV-liposome fusion of any one of E1-E3, wherein the nucleic acid probe comprises 5' [detectable label]-[nucleic acid linker]-[quencher] 3'.

E5. The liposome or EV-liposome fusion of any one of E1-E4, wherein the detectable label is a fluorophore.

E6. The liposome or EV-liposome fusion of E5, wherein the fluorophore comprises fluorescein amidite (FAM).

E7. The liposome or EV-liposome fusion of any one of E1-E6, wherein the nucleic acid linker comprises both DNA and RNA nucleotides.

E8. The liposome or EV-liposome fusion of E7, wherein the nucleic acid linker comprises DNA-RNA-DNA.

E9. The liposome or EV-liposome fusion of E8, wherein the nucleic acid linker is 5' TAuuGC 3'.

E10. The liposome or EV-liposome fusion of any one of E1-E9, wherein the nucleic acid probe comprises the structure of 5' FAM-TAuuGC- quencher 3'.

E11. The liposome or EV-liposome fusion of any one of E1-E10, wherein the crRNA is complementary to an miRNA biomarker.

E12. The liposome or EV-liposome fusion of E11, wherein the miRNA biomarker is a cancer biomarker.

E13. The liposome or EV-liposome fusion of any one of E1-E12, wherein the Cas13a nuclease is LwaCas13a.

E14. The liposome or EV-liposome fusion of any one of E1-E13, wherein the Cas13a nuclease and the crRNA are present at a concentration of about 100 nM.

E15. An array comprising an immobilized capture moiety and a tumor-derived EV.

E16. The array of E15, comprising an immobilized capture moiety and a tumor-derived EV-liposome fusion, wherein the EV-liposome fusion comprises a Cas13a nuclease, a crRNA, and a nucleic acid probe, and wherein the nucleic acid probe comprises a detectable label, a nucleic acid linker, and a quencher.

E17. The array of E15 or E16, wherein the array is a gold microdisk array.

E18. The array of E15 or E16, wherein the array is a gold nanodisk array.

E19. The array of any one of E15-E18, wherein the array comprises a plurality of the immobilized capture moiety.

E20. The array of E19, wherein the immobilized capture moieties on the array are arranged in a grid pattern.

E21. The array of any one of E15-E20, wherein the immobilized capture moiety is an antibody that specifically binds a tumor-derived EV.

E22. The array of E21, wherein the immobilized capture moiety is an antibody that binds EPCAM.

E23. The array of E21, wherein the immobilized capture moiety is an antibody that binds a protein over-expressed in solid tumors.

E24. The array of E23, wherein the immobilized capture moiety is an antibody that binds EGFR, MUC1, MUC16, CD24, or HER2.

E25. The array of E21, wherein the immobilized capture moiety is an antibody that binds a protein associated with drug resistance (for example, chemotherapy resistance).

E26. The array of E25, wherein the immobilized capture moiety is an antibody that binds poly-glycoprotein or survivin.

E27. A method for detecting an miRNA biomarker in a tumor-derived EV, the method comprising detecting the miRNA biomarker in the EV-liposome fusion of any one of E2-E14.

E28. A method for detecting an miRNA biomarker in a tumor-derived EV, comprising the steps of: (a) providing an array comprising a plurality of immobilized capture moieties that specifically bind a tumor-derived EV; (b) binding the tumor-derived EVs to the array; (c) incubating the bound tumor-derived EVs with the liposomes of any one of E1 and E3-E14; and (d) detecting the miRNA biomarker.

E29. A method for detecting an miRNA biomarker in a tumor-derived EV, comprising the steps of: (a) providing an array comprising a plurality of immobilized capture moieties that specifically bind a tumor-derived EV; (b) binding the EV-liposome fusion of any one of E2-E14 to the array; and (c) detecting the miRNA biomarker.

E30. The method of any one of E27-E29, wherein the biomarker is a cancer biomarker.

E31. The method of any one of E28-E30, wherein the array is a gold microdisk array.

E32. The method of any one of E28-E30, wherein the array is a gold nanodisk array.

E33. The method of any one of E28-E32, wherein the array comprises a plurality of immobilized capture moieties arranged in a grid pattern.

E34. The method of any one of E28-E33, wherein the immobilized capture moiety is an antibody that specifically binds a tumor-derived EV.

E35. The method of E34, wherein the immobilized capture moiety is an antibody that binds EPCAM.

E36. The method of E34, wherein the immobilized capture moiety is an antibody that binds a protein that is over-expressed in solid tumors.

E37. The method of E36, wherein the immobilized capture moiety is an antibody that binds EGFR, MUC1, MUC16, CD24, or HER2.

E38. The method of E34, wherein the immobilized capture moiety is an antibody that binds a protein associated with drug resistance.

E39. The method of E38, wherein the immobilized capture moiety is an antibody that binds poly-glycoprotein or survivin.

E40. The method of any one of E27-E39, wherein the method further comprises detecting one or more proteins on the EV-liposome fusion by immunolabeling.

E41. The method of E40, wherein the one or more proteins are over-expressed in solid tumors.

E42. The method of E41, wherein the one or more proteins comprises EGFR, MUC1, MUC16, CD24, or HER2.

E43. The method of E40, wherein the one or more proteins are associated with drug resistance.

E44. The method of E43, wherein the one or more proteins comprises poly-glycoprotein or survivin.

Other embodiments are within the following claims.

CLAIMS

1. A liposome comprising a Cas13a nuclease, a crRNA, and a nucleic acid probe, wherein the nucleic acid probe comprises a detectable label, a nucleic acid linker, and a quencher.

2. An extracellular vesicle-liposome (EV-liposome) fusion comprising a Cas13a nuclease, a crRNA, and a nucleic acid probe, wherein the nucleic acid probe comprises a detectable label, a nucleic acid linker, and a quencher.

3. The liposome of claim 1 or the EV-liposome fusion of claim 2, wherein the EV is a tumor-derived EV.

4. The liposome of claim 1 or the EV-liposome fusion of claim 2, wherein the nucleic acid probe comprises 5' [detectable label]-[nucleic acid linker]-[quencher] 3'.

5. The liposome of claim 1 or the EV-liposome fusion of claim 2, wherein the detectable label is a fluorophore.

6. The liposome or EV-liposome fusion of claim 5, wherein the fluorophore comprises fluorescein amidite (FAM).

7. The liposome of claim 1 or the EV-liposome fusion of claim 2, wherein the nucleic acid linker comprises both DNA and RNA nucleotides.

8. The liposome or EV-liposome fusion of claim 7, wherein the nucleic acid linker comprises DNA-RNA-DNA.

9. The liposome or EV-liposome fusion of claim 8, wherein the nucleic acid linker is 5' TAuuGC 3'.

10. The liposome of claim 1 or the EV-liposome fusion of claim 2, wherein the nucleic acid probe comprises the structure of 5' FAM-TAuuGC- quencher 3'.

11. The liposome of claim 1 or the EV-liposome fusion of claim 2, wherein the crRNA is complementary to an miRNA biomarker.

12. The liposome or EV-liposome fusion of claim 11, wherein the miRNA biomarker is a cancer biomarker.

13. The liposome of claim 1 or the EV-liposome fusion of claim 2, wherein the Cas13a nuclease is LwaCas13a.

14. The liposome of claim 1 or the EV-liposome fusion of claim 2, wherein the Cas13a nuclease and the crRNA are present at a concentration of about 100 nM.

15. An array comprising an immobilized capture moiety and a tumor-derived EV.

16. The array of claim 15, comprising an immobilized capture moiety and a tumor-derived EV-liposome fusion, wherein the EV-liposome fusion comprises a Cas13a nuclease, a crRNA, and a nucleic acid probe, and wherein the nucleic acid probe comprises a detectable label, a nucleic acid linker, and a quencher.

17. The array of claim 15, wherein the array is a gold microdisk array.

18. The array of claim 15, wherein the array is a gold nanodisk array.

19. The array of claim 15, wherein the array comprises a plurality of the immobilized capture moiety.

20. The array of claim 19, wherein the immobilized capture moieties on the array are arranged in a grid pattern.

21. The array of claim 15, wherein the immobilized capture moiety is an antibody that specifically binds a tumor-derived EV.

22. The array of claim 21, wherein the immobilized capture moiety is an antibody that binds EPCAM.

23. The array of claim 21, wherein the immobilized capture moiety is an antibody that binds a protein over-expressed in solid tumors.

24. The array of claim 23, wherein the immobilized capture moiety is an antibody that binds EGFR, MUC1, MUC16, CD24, or HER2.

25. The array of claim 21, wherein the immobilized capture moiety is an antibody that binds a protein associated with drug resistance (for example, chemotherapy resistance).

26. The array of claim 25, wherein the immobilized capture moiety is an antibody that binds poly-glycoprotein or survivin.

27. A method for detecting an miRNA biomarker in a tumor-derived EV, the method comprising detecting the miRNA biomarker in the EV-liposome fusion of claim 2.

28. A method for detecting an miRNA biomarker in a tumor-derived EV, comprising the steps of:

(a) providing an array comprising a plurality of immobilized capture moieties that specifically bind a tumor-derived EV;

(b) binding the tumor-derived EVs to the array;

(c) incubating the bound tumor-derived EVs with the liposomes of claim 1; and

(d) detecting the miRNA biomarker.

29. A method for detecting an miRNA biomarker in a tumor-derived EV, comprising the steps of:

(a) providing an array comprising a plurality of immobilized capture moieties that specifically bind a tumor-derived EV;

(b) binding the EV-liposome fusion of claim 2 to the array; and

(c) detecting the miRNA biomarker.

30. The method of any one of claims 27-29, wherein the biomarker is a cancer biomarker.

31. The method of claim 28 or 29, wherein the array is a gold microdisk array.

32. The method of claim 28 or 29, wherein the array is a gold nanodisk array.

33. The method of claim 28 or 29, wherein the array comprises a plurality of immobilized capture moieties arranged in a grid pattern.

34. The method of claim 28 or 29, wherein the immobilized capture moiety is an antibody that specifically binds a tumor-derived EV.

35. The method of claim 34, wherein the immobilized capture moiety is an antibody that binds EPCAM.

36. The method of claim 34, wherein the immobilized capture moiety is an antibody that binds a protein that is over-expressed in solid tumors.

37. The method of claim 36, wherein the immobilized capture moiety is an antibody that binds EGFR, MUC1, MUC16, CD24, or HER2.

38. The method of claim 34, wherein the immobilized capture moiety is an antibody that binds a protein associated with drug resistance.

39. The method of claim 38, wherein the immobilized capture moiety is an antibody that binds poly-glycoprotein or survivin.

40. The method of any one of claims 27-29, wherein the method further comprises detecting one or more proteins on the EV-liposome fusion by immunolabeling.

41. The method of claim 40, wherein the one or more proteins are over-expressed in solid tumors.

42. The method of claim 41, wherein the one or more proteins comprises EGFR, MUC1, MUC16, CD24, or HER2.

43. The method of claim 40, wherein the one or more proteins are associated with drug resistance.

44. The method of claim 43, wherein the one or more proteins comprises poly-glycoprotein or survivin.

FIG. 1

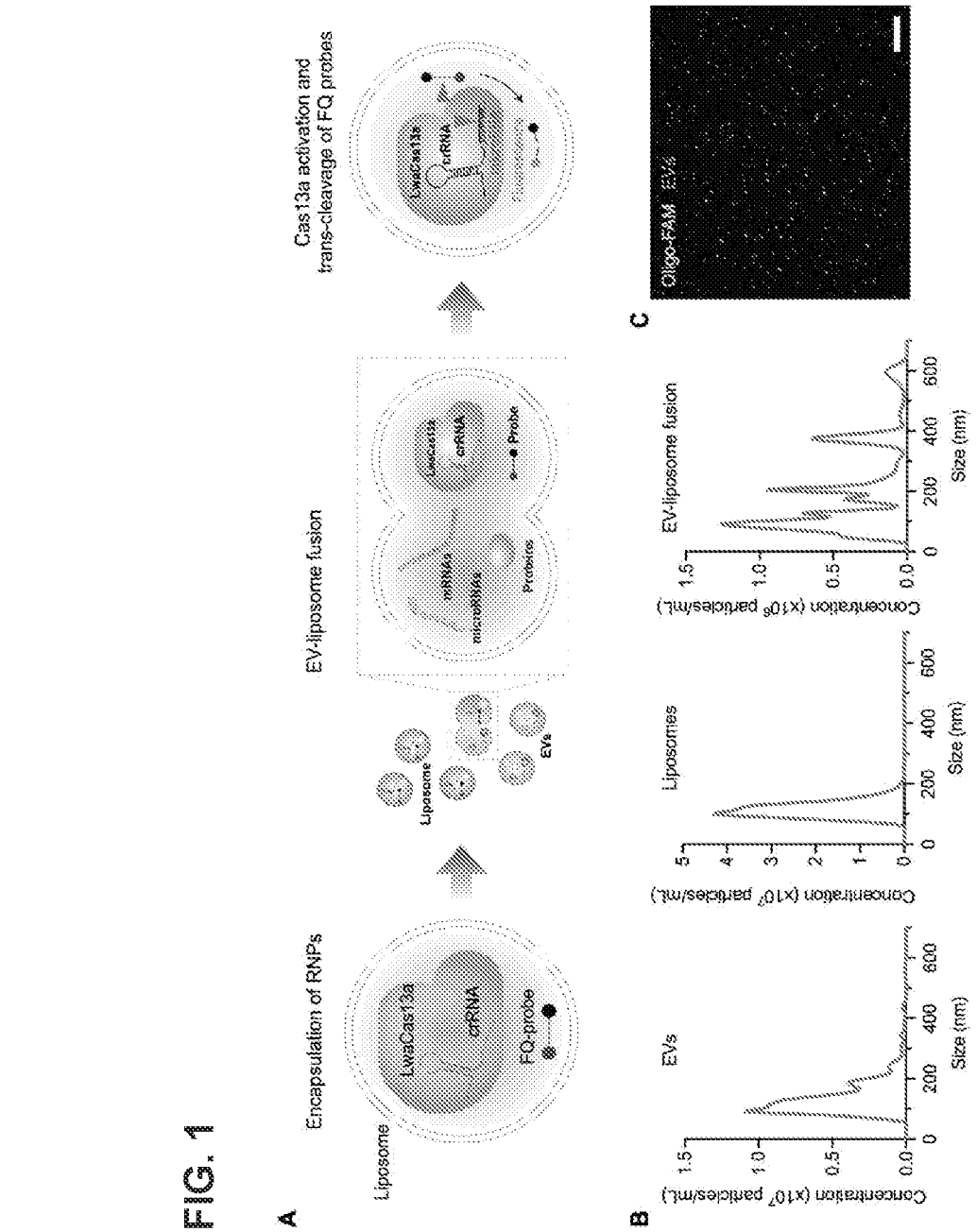
A
Encapsulation of RNPs
Liposome
LwaCas13a
crRNA
FQ-probe
Liposome
EVs
EV-liposome fusion
mRNAs
microRNAs
Proteins
Cas13a
crRNA
Probe
Cas13a activation and
trans-cleavage of FQ probes
B
EVs
Liposomes
EV-liposome fusion
Concentration (x10⁷ particles/mL)
Concentration (x10⁶ particles/mL)
Size (nm)
C
Oligo-FAM
EVs

FIG. 2

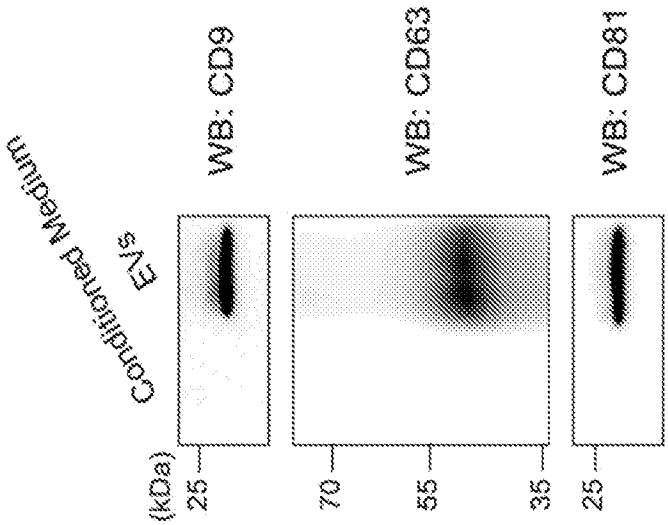
Conditioned Medium
EVs
WB: CD9
WB: CD63
WB: CD81
(kDa)
25
70
55
35
25

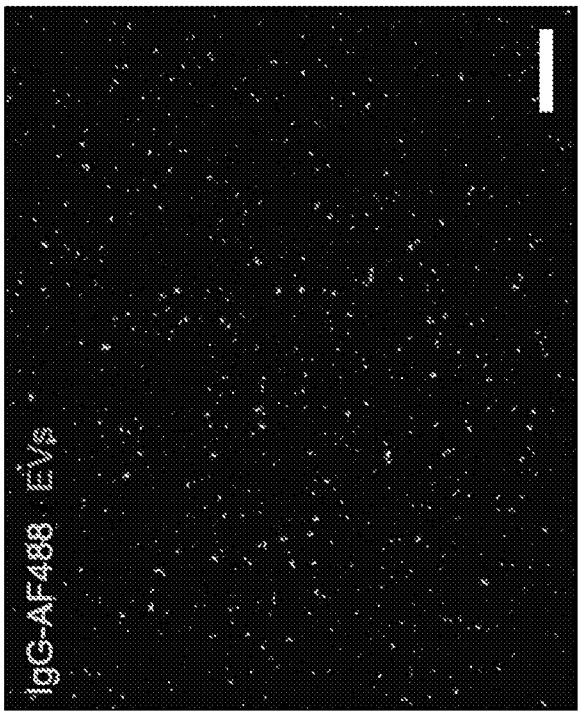

FIG. 3

FIG. 4

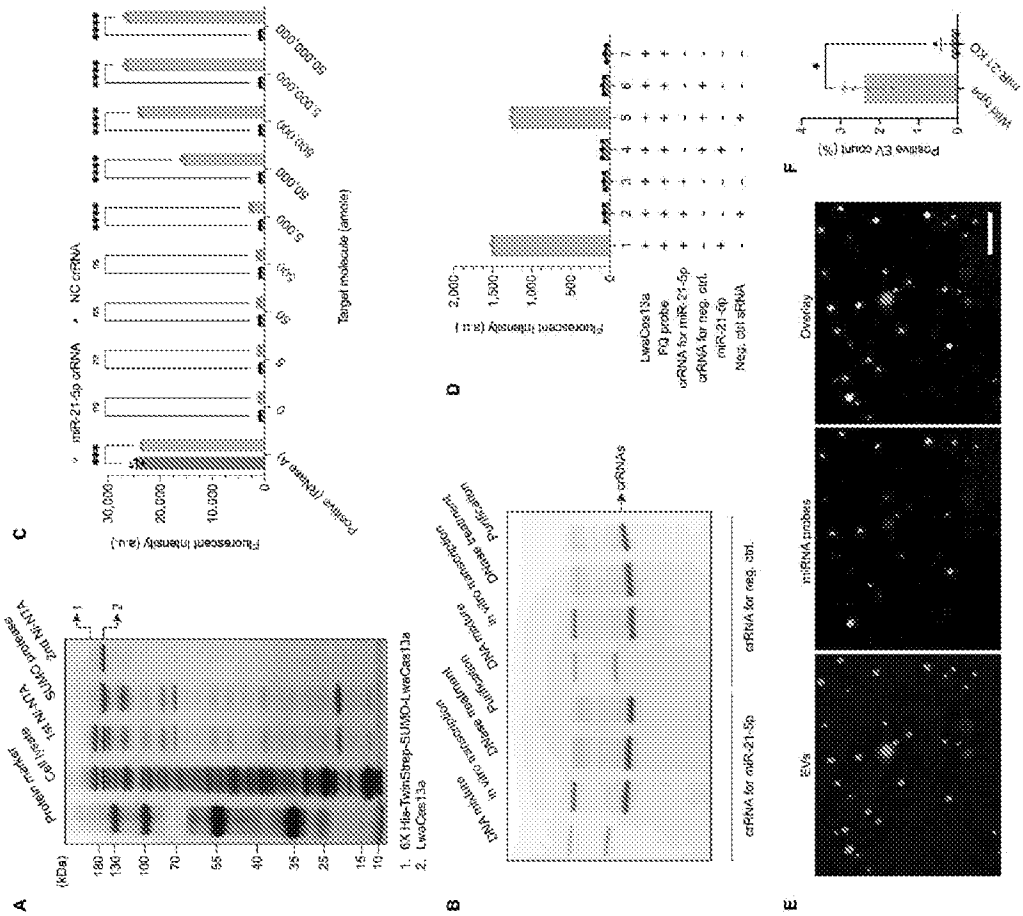
A
(kDa)
180
130
100
70
55
40
35
25
15
10
Protein marker
Cell lysate
1st Ni-NTA
SUMO protease
2nd Ni-NTA
1. 6X His-TwinStrep-SUMO-LwaCas13a
2. LwaCas13a
B
DNA template
In vitro transcription
Digest reaction
Purification
Dilute mixture
In vitro transcription
Digest reaction
Purification
crRNAs
crRNA for miR-21-5p
crRNA for neg. ctrl.
C
miR-21-5p crRNA
NC crRNA
Fluorescent intensity (a.u.)
30,000
20,000
10,000
0
Positive (Replica A)
Target molecule (amole)
0
5
50
500
5,000
50,000
500,000
5,000,000
50,000,000
D
Fluorescent intensity (a.u.)
2,000
1,500
1,000
500
0
LwaCas13a
FQ probe
crRNA for miR-21-5p
crRNA for neg. ctrl.
miR-21-5p
Neg. ctrl sRNA
E
EVs
miRNA probes
Overlay
F
Positive EV count (%)
4
3
2
1
0
Wild type
miR-21 KO

FIG. 5

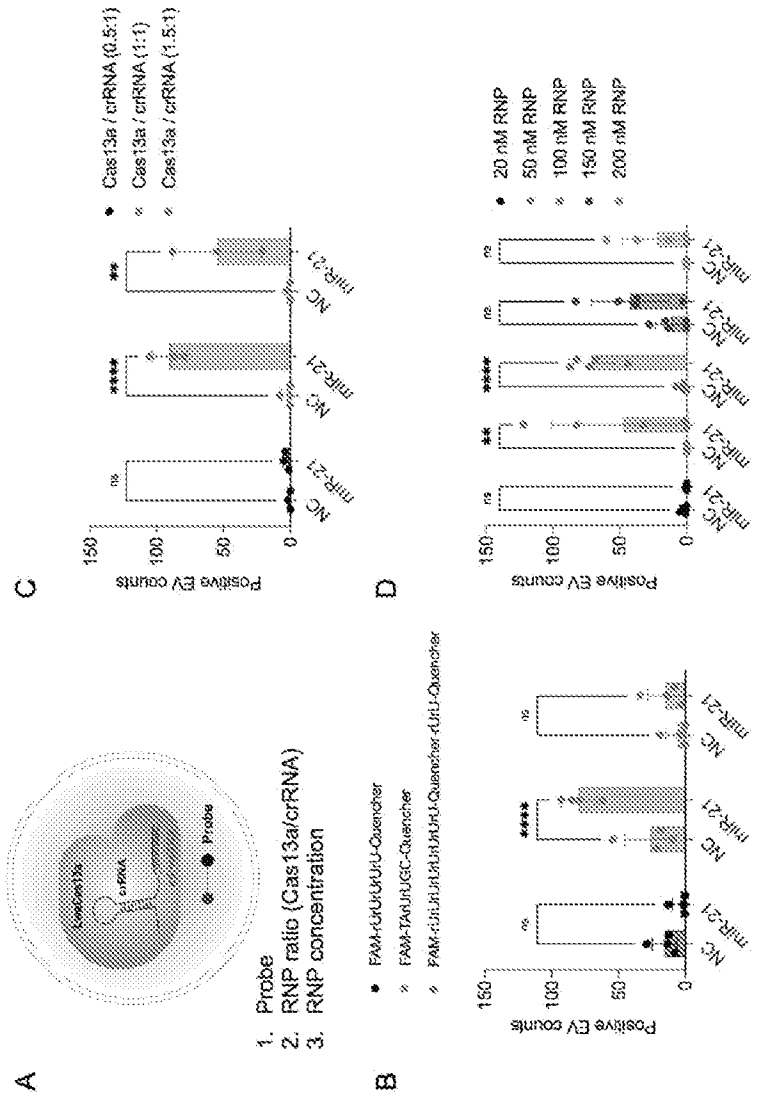
A
Cas13a
crRNA
Probe
1. Probe
2. RNP ratio (Cas13a/crRNA)
3. RNP concentration
B
FAM-rUrUrUrU-Quencher
FAM-TArUrUGC-Quencher
FAM-rUrUrUrUrUrU-Quencher-rUrU-Quencher
Positive EV counts
NC
miR-21
C
Cas13a / crRNA (0.5:1)
Cas13a / crRNA (1:1)
Cas13a / crRNA (1.5:1)
ns
**
****
D
20 nM RNP
50 nM RNP
100 nM RNP
150 nM RNP
200 nM RNP

FIG. 6

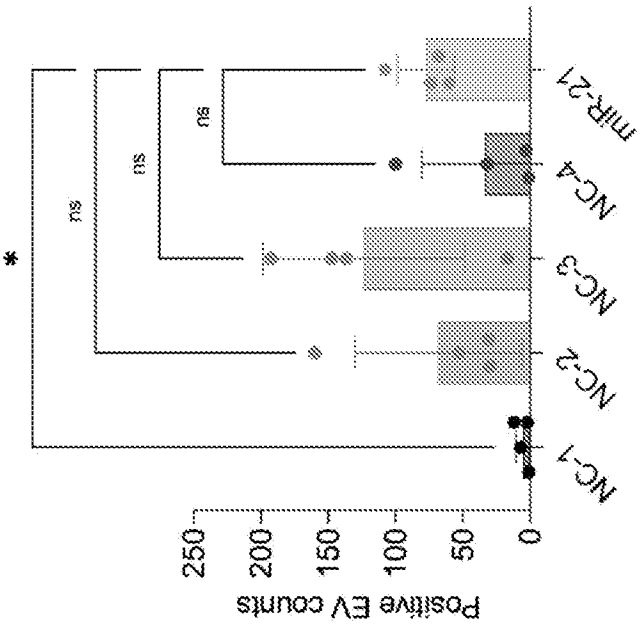
Positive EV counts
250
200
150
100
50
0
NC-1
NC-2
NC-3
NC-4
miR-21
*
ns
ns
ns

FIG. 7

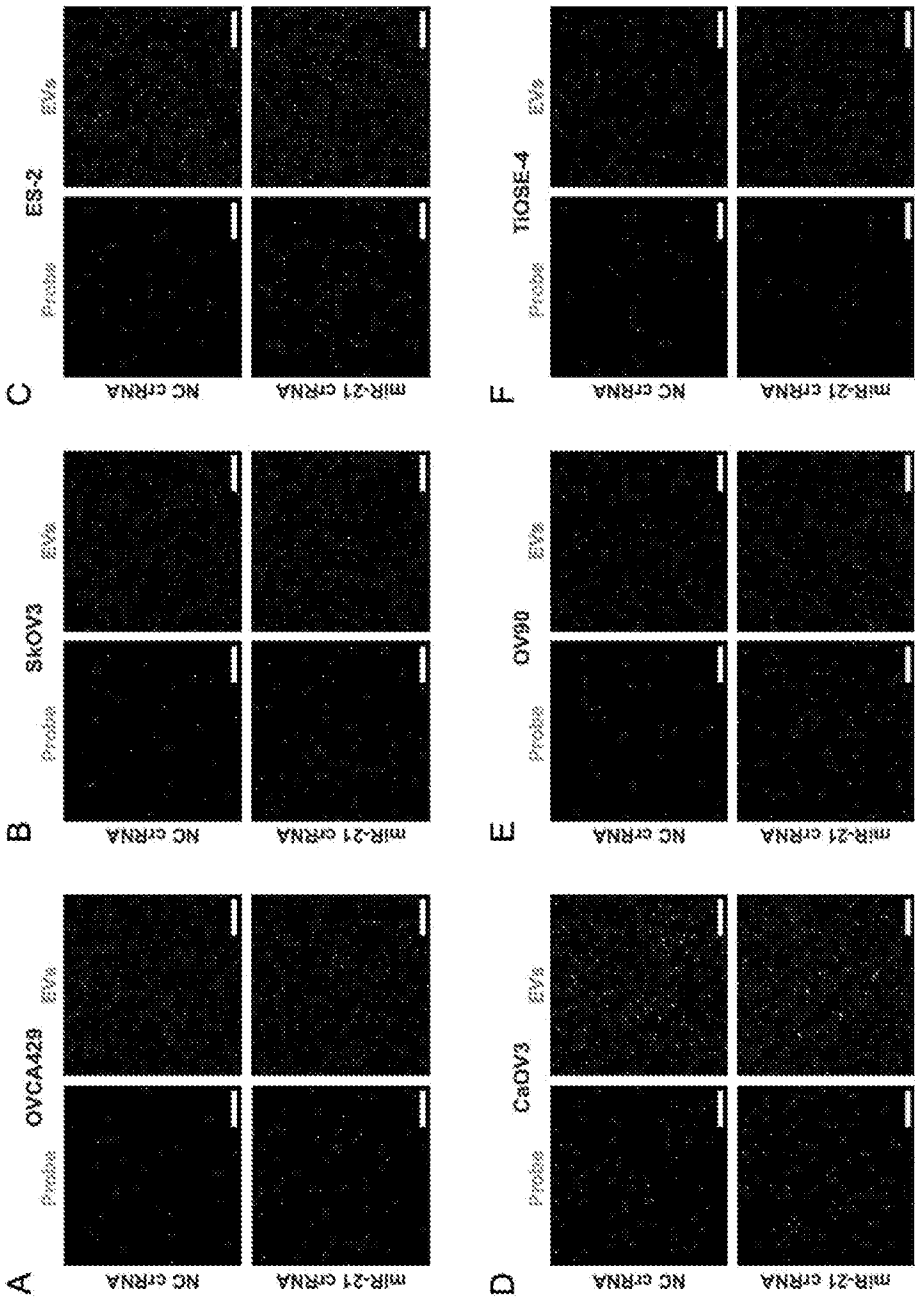
A
OVCA429
Probe
EVs
NC crRNA
miR-21 crRNA
B
SKOV3
C
ES-2
D
CaOV3
E
OV90
F
TIOSE-4

FIG. 8

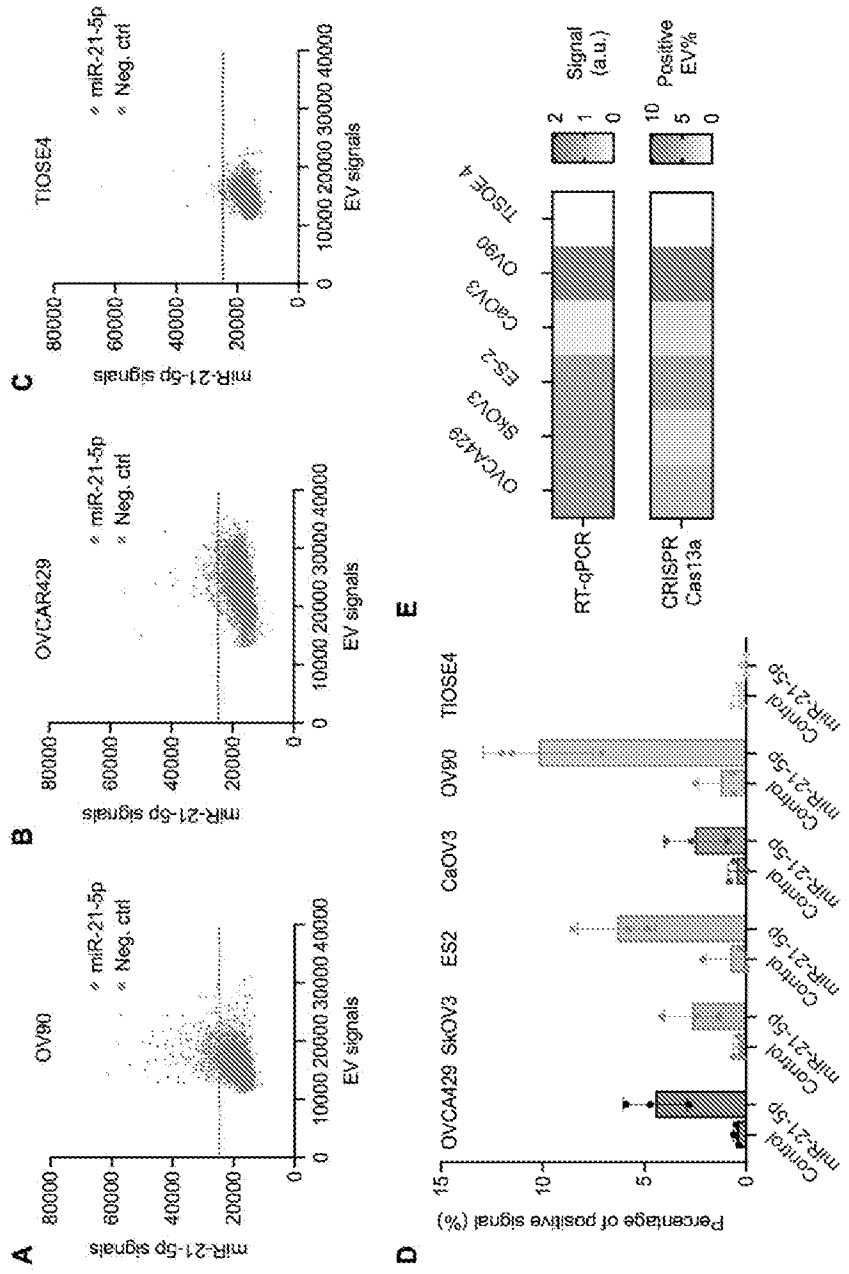
A
OV90
miR-21-5p
Neg. ctrl
miR-21-5p signals
EV signals
B
OVCAR429
C
TIOSE4
D
Percentage of positive signal (%)
OVCA429
SkOV3
ES2
CaOV3
OV90
TIOSE4
Control
miR-21-5p
E
RT-qPCR
CRISPR Cas13a
Signal (a.u.)
Positive EV%

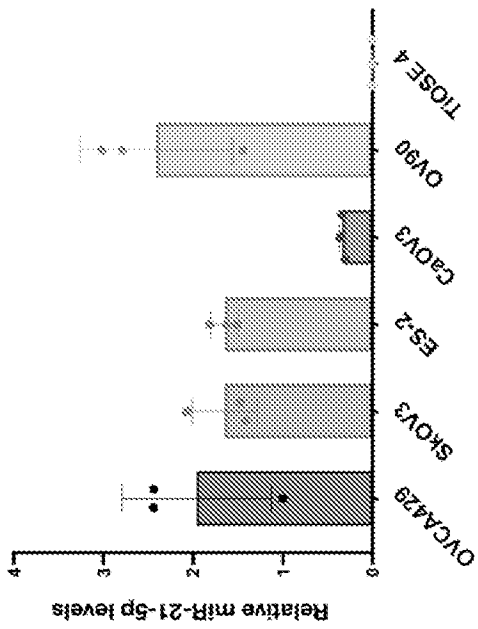
Relative miR-21-5p levels
0
1
2
3
4
OVCA429
SKOV3
ES-2
CaOV3
OV90
TIOSE4

FIG. 9

FIG. 10

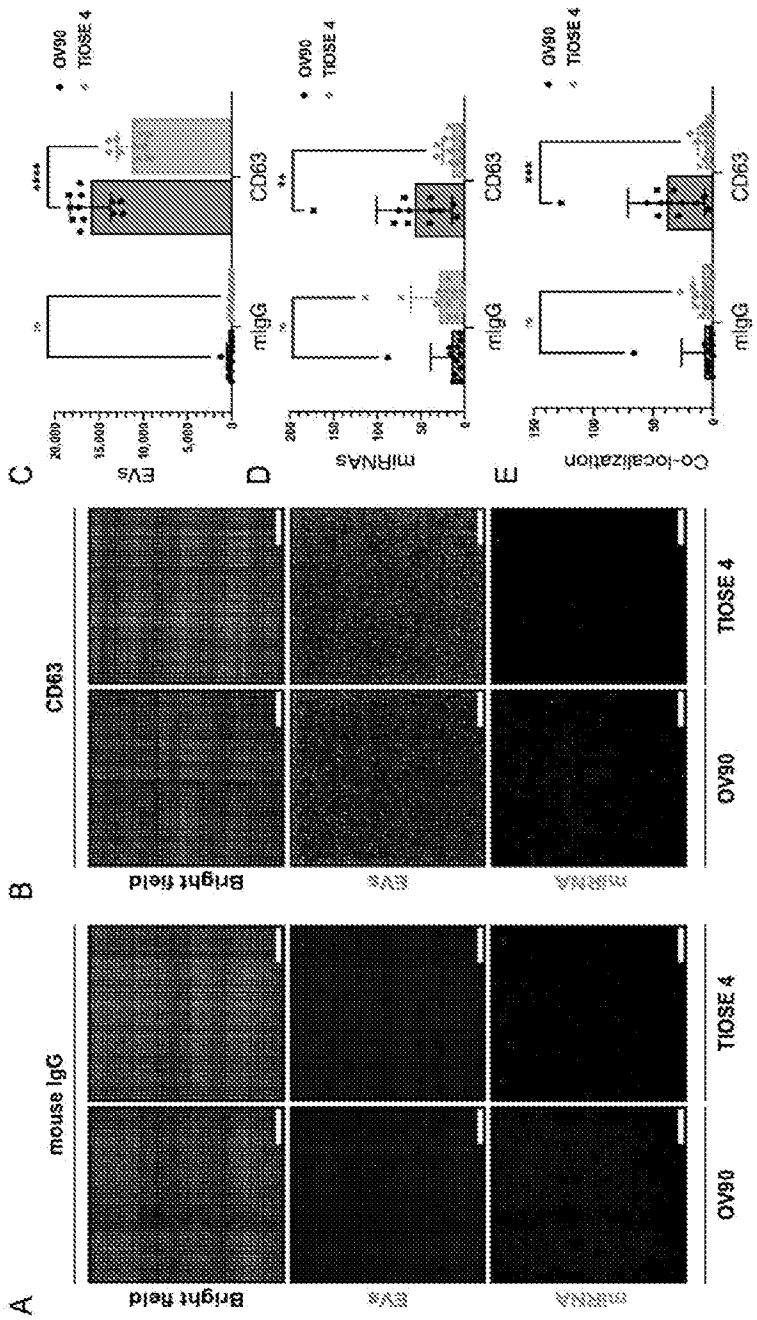
A
mouse IgG
OV90
TIOSE 4
Bright field
EVs
mRNA
B
CD63
OV90
TIOSE 4
Bright field
EVs
mRNA
C
EVs
OV90
TIOSE 4
mIgG
CD63
D
miRNAs
OV90
TIOSE 4
mIgG
CD63
E
Co-localization
OV90
TIOSE 4
mIgG
CD63

FIG. 11

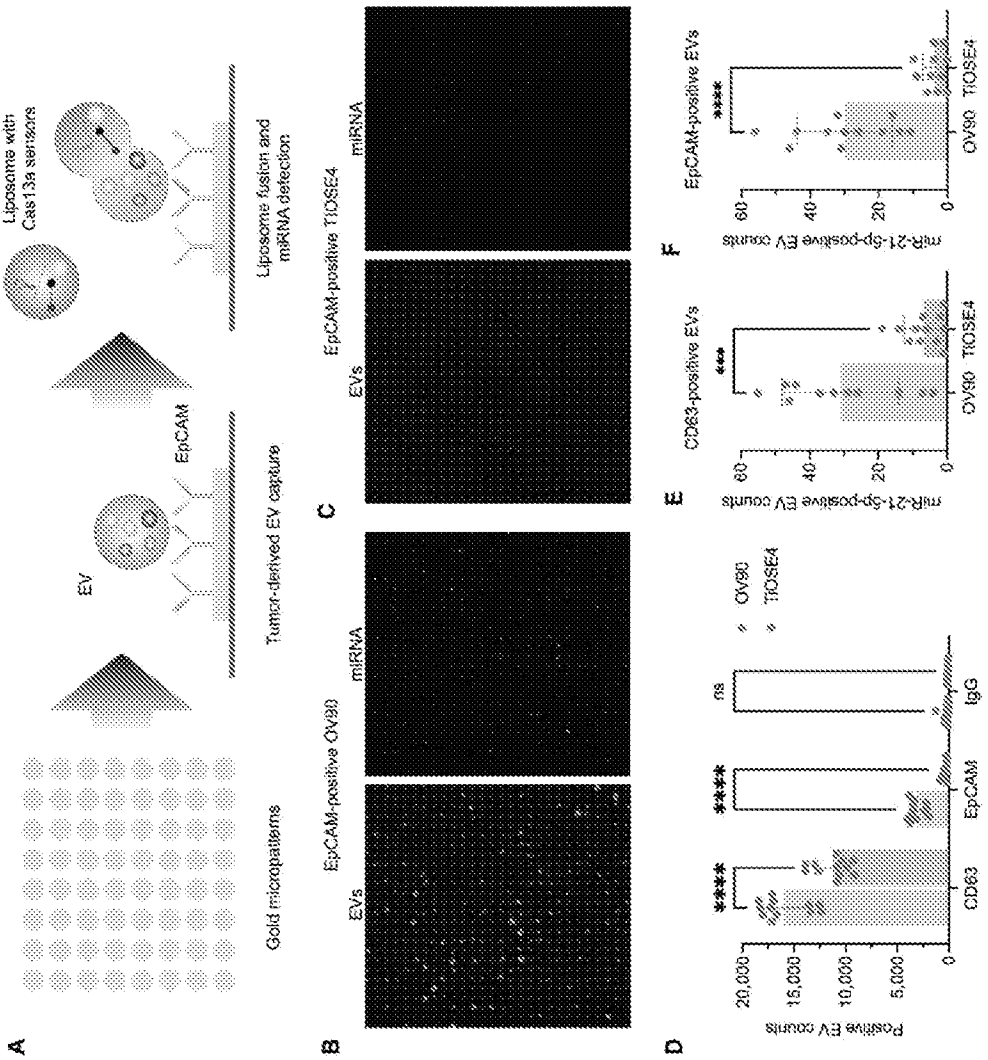
A
Liposome with Cas13a sensors
EV
EpCAM
Gold micropatterns
Tumor-derived EV capture
Liposome fusion and miRNA detection
B
EpCAM-positive OV90
EVs
miRNA
C
EpCAM-positive TIOSE4
EVs
miRNA
D
Positive EV counts
20,000
15,000
10,000
5,000
0
****
****
ns
CD63
EpCAM
IgG
OV90
TIOSE4
E
CD63-positive EVs
***
miR-21-5p-positive EV counts
60
40
20
0
OV90
TIOSE4
F
EpCAM-positive EVs
****
miR-21-5p-positive EV counts
60
40
20
0
OV90
TIOSE4

FIG. 12

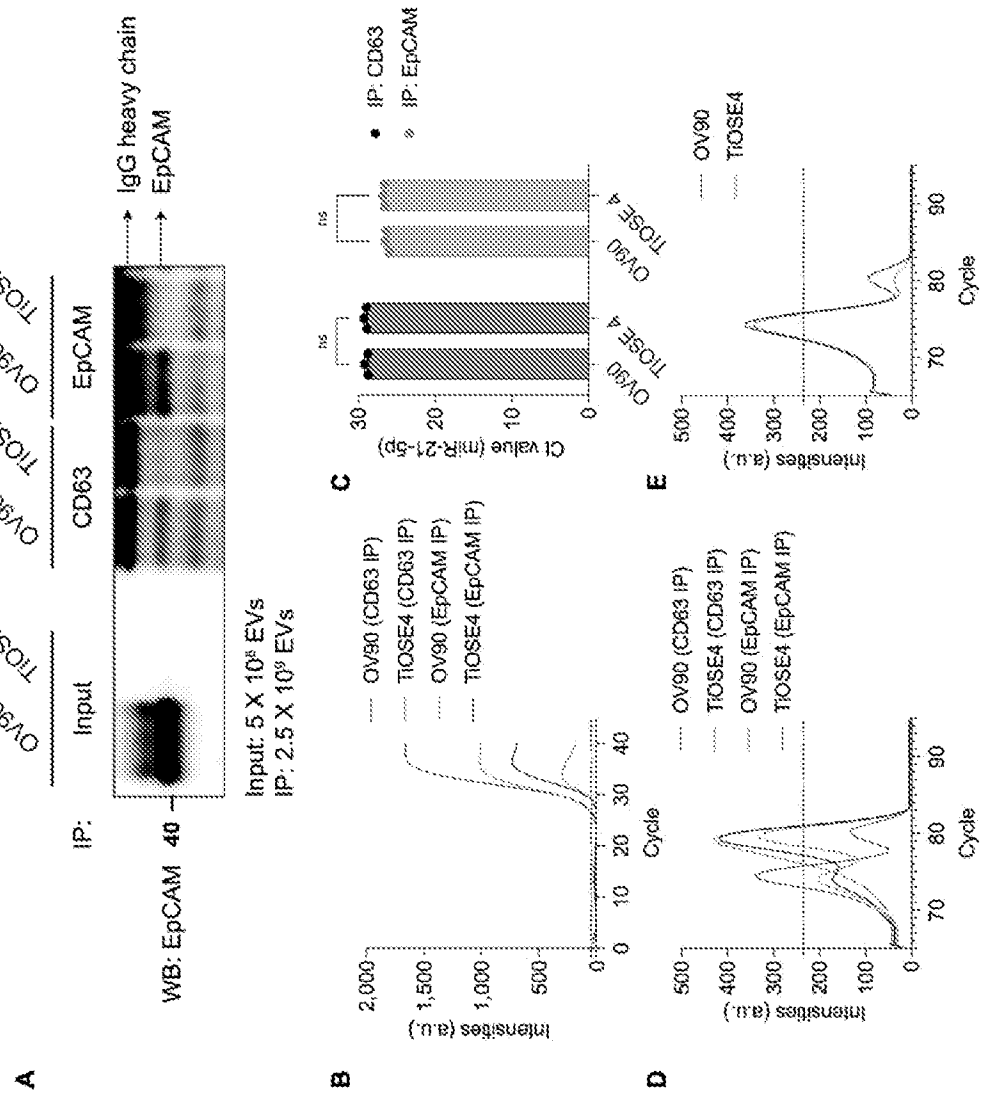
A
IP:
Input
CD63
EpCAM
OV90
TtOSE4
OV90
TtOSE4
OV90
TtOSE4
IgG heavy chain
EpCAM
WB: EpCAM
40
Input: 5 X 10⁵ EVs
IP: 2.5 X 10⁵ EVs
B
OV90 (CD63 IP)
TtOSE4 (CD63 IP)
OV90 (EpCAM IP)
TtOSE4 (EpCAM IP)
Intensities (a.u.)
Cycle
C
IP: CD63
IP: EpCAM
Ct value (miR-21-5p)
ns
ns
OV90
TtOSE 4
OV90
TtOSE 4
D
OV90 (CD63 IP)
TtOSE4 (CD63 IP)
OV90 (EpCAM IP)
TtOSE4 (EpCAM IP)
Intensities (a.u.)
Cycle
E
OV90
TtOSE4
Intensities (a.u.)
Cycle